Heme iron amplifies azoxymethane initiating effect on rat colon preneoplastic lesions

Julia Keller, Pascale Plaisancié, Edwin Fouché, Edwige-Marie Pralet, Nathalie Naud, Blas-Y-Estrada F, Claire Maslo, Ingrid Ahn, Sylvie Chevolleau, Maria-Helena Meireles, et al.

▶ **To cite this version:**

Julia Keller, Pascale Plaisancié, Edwin Fouché, Edwige-Marie Pralet, Nathalie Naud, et al.. Heme iron amplifies azoxymethane initiating effect on rat colon preneoplastic lesions. Redox Experimental Medicine, 2025, 2025 (1), pp.e250001. ⟨10.1530/REM-25-0001⟩. ⟨hal-04976816v2⟩

HAL Id: hal-04976816

https://hal.science/hal-04976816v2

Submitted on 22 Jul 2025

HAL is a multi-disciplinary open access archive for the deposit and dissemination of scientific research documents, whether they are published or not. The documents may come from teaching and research institutions in France or abroad, or from public or private research centers.

L'archive ouverte pluridisciplinaire **HAL**, est destinée au dépôt et à la diffusion de documents scientifiques de niveau recherche, publiés ou non, émanant des établissements d'enseignement et de recherche français ou étrangers, des laboratoires publics ou privés.

Distributed under a Creative Commons CC BY-NC-ND 4.0 - Attribution - Non-commercial use - No Derivative Works - International License

Redox Experimental Medicine (2025) **2025** e250001
https://doi.org/10.1530/REM-25-0001

Received 8 January 2025
Accepted 11 February 2025
Available online 11 February 2025
Version of Record published 26 February 2025

RESEARCH

Heme iron amplifies azoxymethane initiating effect on rat colon preneoplastic lesions

Julia Keller[1,*], Pascale Plaisancié[1,*], Edwin Fouché[1], Edwige-Marie Pralet[1], Nathalie Naud[1], Florence Blas-Y-Estrada[1], Claire Maslo[1], Ingrid Ahn[1], Sylvie Chevolleau[1,2], Maria-Helena Meireles[1,2], Cécile Héliès-Toussaint[1], Sylvia Pietri[3], Mathieu Cassien[3], Laure Khoury[4], Marc Audebert[1], Fabrice Pierre[1], Vassilia Theodorou[1], Maïwenn Olier[1] and Françoise Guéraud[1]

[1]Toxalim (Research Centre in Food Toxicology), Toulouse University, INRAE UMR 1331, ENVT, INP-Purpan, Paul Sabatier University, Toulouse, France
[2]Metatoul-AXIOM platform, MetaboHUB-MetaToul, National Infrastructure for Metabolomics and Fluxomics: MetaboHUB, Toulouse, France
[3]Aix Marseille University, CNRS, ICR, SMBSO, Marseille, France
[4]PrediTox, 1 place Pierre Potier, Toulouse, France

Correspondence should be addressed to F Guéraud: francoise.gueraud@inrae.fr

*(J Keller and P Plaisancié contributed equally to this work)

Graphical abstract

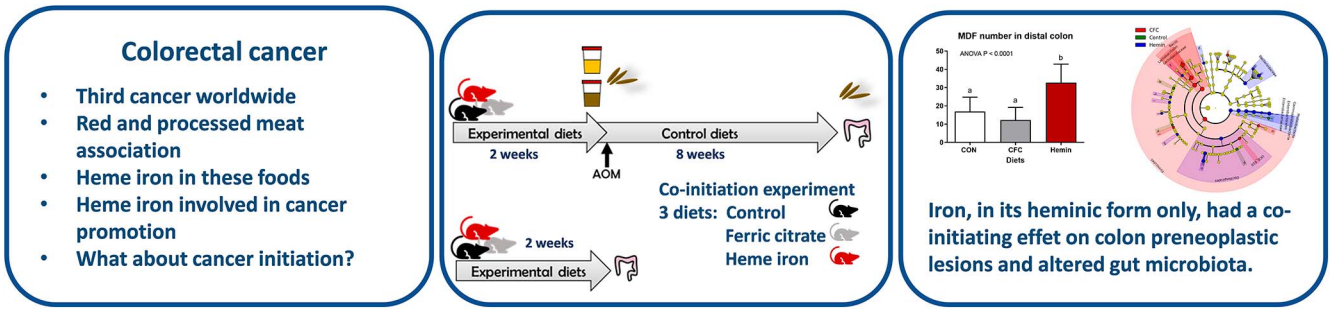

Abstract

Objective: Colorectal cancer is a major public health issue for which dietary factors such as red and processed meat consumption seem to play a prominent role. Heme iron, which is present in important concentration in those food products, was reported to play a role in colorectal cancer promotion in animal studies. However, its role in colorectal cancer initiation remains to be established.

Methods: Male Fischer 344 rats were given experimental diets (control diet, ferric citrate-supplemented diet or hemin-supplemented diet) for 2 weeks before being initiated for colon cancer with azoxymethane. Rats were then fed a control diet for 8 weeks. Preneoplastic lesions, lipid peroxidation, genotoxicity and oxidative stress markers, together with gut microbiota, were analyzed.

Results: Heme iron, given in the rat diet for only 2 weeks before the colorectal cancer initiating event, increased two types of preneoplastic lesions in the rat colon, namely aberrant crypt foci and mucin-depleted foci, when compared to a control

Published by Bioscientifica Ltd.
https://rem.bioscientifica.com
© 2025 the author(s)

This work is licensed under a Creative Commons Attribution-NonCommercial-NoDerivatives 4.0 International License.

Downloaded from Bioscientifica.com at 07/22/2025 01:00:31PM
via Open Access. This work is licensed under a Creative Commons Attribution-NonCommercial-NoDerivatives 4.0 International License.
https://creativecommons.org/licenses/by-nc-nd/4.0/

Redox Experimental Medicine (2025) **2025** e250001
https://doi.org/10.1530/REM-25-0001

diet containing the same amount of iron in a non-heminic form. This heme iron concentration in the diet, representative of human consumption, induced at the same time a huge increase in luminal lipid peroxidation, a significant increase in RNA/DNA oxidative damage and an increase in the expression of antioxidant defenses in colon mucosa, accompanied by epithelial cell proliferation together with a reduction in colon mucus cells, and a gut dysbiosis.

Conclusion: These results, obtained in an animal model, suggest that iron, only in its heminic form, has a co-initiating effect on colorectal carcinogenesis.

Significance statement

Heme iron from red meat could play a role in colon cancer initiation in addition to its promoting effect.

Keywords: red meat; colorectal cancer initiation; heme iron; lipid peroxidation; gut dysbiosis

Introduction

Cancer is the first cause of premature mortality in the most developed countries. Colorectal cancer (CRC) is a leading cause of cancer-related death in men and women. Its incidence is much higher in transitioned versus transitioning countries (Bray *et al.* 2018). Based on meta-analyses, the World Cancer Research Fund (WCRF) classified the evidence of an association between red and processed meat consumption and the risk to develop CRC as probable and convincing, respectively (Clinton *et al.* 2020). The International Agency for Research on Cancer (IARC) from the World Health Organization (WHO) has classified processed meat as 'carcinogenic to humans' (Group 1) and red meat as 'probably carcinogenic to humans' (Group 2A) (Bouvard *et al.* 2015, IARC Working Group on the Evaluation of Carcinogenic Risk to Humans 2018), mostly based on their effect on CRC risk. Heme iron, a particular form of dietary iron of animal origin, is present in high concentration in red and processed meats, giving red and pink (nitrosyl-heme) color to those meats, respectively. Our group and others have identified heme iron as a key element in the mechanism linking red and processed meat and CRC development (Sesink *et al.* 1999, 2001, Pierre *et al.* 2003, 2004, Bastide *et al.* 2015). Heme iron is a pro-oxidant compound that catalyzes the peroxidation of nutrients, particularly of polyunsaturated fatty acids in the intestinal lumen during digestion, generating a cancer-promoting environment in the colon (Guéraud *et al.* 2015). Indeed, this luminal peroxidation gives rise to cytotoxic and genotoxic lipid peroxidation products such as malondialdehyde and 4-hydroxynonenal (HNE), which are absorbed and partially metabolized by epithelial cells. This implication of luminal heme iron and lipid oxidation products has been reinforced by an epidemiological study in which the risk of developing colon adenoma was no longer associated with heme iron intake when dietary total antioxidant capacity was high (Bastide *et al.* 2016), emphasizing the role of oxidative processes. In the same line, WCRF concluded in 2018 that the consumption of foods containing heme iron might increase the risk of CRC (Clinton *et al.* 2020).

The promoting effect of heme iron on colorectal carcinogenesis has been evidenced in animal model studies, in azoxymethane- (AOM) or dimethylhydrazine-initiated rats or in Min mice (Multiple intestinal neoplasia, due to a mutation on the *Apc* gene), in which heme iron, red- or processed-meat-rich diets induced more preneoplastic lesions (rats) or more tumors (mice) than a control diet (Pierre *et al.* 2003, 2004, 2008, Bastide *et al.* 2015, Constante *et al.* 2017, Martin *et al.* 2018). In these experiments, the promoting effect of heme iron was tested after the colon carcinogenesis-initiating event, such as AOM treatment for rats or loss of heterozygosity in *Apc*-mutated mice (Min mice). Apc mutation, considered an early and frequent event in human colorectal carcinogenesis, is observed in adenoma in Min mice and preneoplastic lesions such as mucin-depleted foci (MDF) in rats. To the best of our knowledge, no experiments were performed in animal models to study the effect of heme iron on colon cancer initiation. In the present paper, we tested the co-initiating properties of heme iron, given to rats in their diet for only 2 weeks before the colon carcinogenesis-initiating event (AOM injection), compared to an equimolar ferric citrate diet or an iron non-supplemented diet. Rats were then fed normal diets for 60 days in order to let preneoplastic lesions to develop. Before the AOM-induced carcinogenesis initiation, we found that heme iron feeding was associated with modulations of colon antioxidant defenses, epithelial colon cell proliferation and gut dysbiosis. After 60 days of normal diet post-AOM injection, we showed that rats fed the heme-iron-containing diet before the carcinogenesis-initiating event had significantly more of two types of preneoplastic lesions in their colon than their counterparts fed a normal or ferric citrate-supplemented diet throughout the experimental diet period.

Downloaded from Bioscientifica.com at 07/22/2025 01:00:31PM
via Open Access. This work is licensed under a Creative Commons
Attribution-NonCommercial-NoDerivatives 4.0 International License.
https://creativecommons.org/licenses/by-nc-nd/4.0/

Redox Experimental Medicine (2025) **2025** e250001
https://doi.org/10.1530/REM-25-0001

Materials and methods

Animals and diets

Ethical approval

The animal experiment was approved by the local Ethical Committee (CE no. 86), authorized by the French Ministry of Research (TOXCOM/0007-0010/FG and TOXCOM/0175/FG APAFiS #8600) and conducted in accordance with the European Union and ARRIVE guidelines.

Animals

Male Fischer 344 (F344/IcoCrl) rats (28 rats/group) were purchased from Charles River Laboratories at 4 weeks of age. After acclimatization, the animals were randomly assigned to the experimental diet groups and fed those diets for 2 weeks. Eight rats per group were then euthanized to evaluate immediate diet effects on colon or blood parameters, while the other 20 rats per group were IP injected with 20 mg/kg AOM in NaCl 9 g/L (Sigma-Aldrich, France) in saline solution and further fed their respective control diet (without supplementary ferric citrate for the CON group and with ferric citrate for the CFC and Hemin groups) for 60 days and then euthanized to evaluate carcinogenesis parameters. Colon, liver and blood were harvested and rapidly processed for further analyses. Urine and feces were collected in plastic metabolic cages during the experimental diet period for lipid peroxidation analysis. Anal feces for microbiota analysis were collected at the end of the experimental diet period and at the end of the whole protocol for the AOM-treated rats.

Experimental diets

Experimental diets were based on powdered, low-calcium, no-fat AIN-76 rodent diets (UPAE, Jouy-en-Josas, France), supplemented with 5% safflower oil (MPBio) (CON diet) and with 0.036% ferric citrate (CFC diet) or with 0.094% hemin (Hemin diet) (Sigma-Aldrich). Hemin was solubilized into safflower oil before being mixed with the powdered modified AIN-76 diet. Ferric citrate was added directly in the powder. After these steps, diets were immediately aliquoted in 1-day portions (40 g for 2 rats), vacuum-packed and frozen until distribution to the animals. Animals were given their diet each day at the end of the afternoon, just before their active period. All these precautions aimed at avoiding any important oxidative degradation.

Both CFC and hemin diets were balanced for iron content, provided in its heminic form in the hemin diet.

Colon histological and immuno-histological analyses

Preneoplastic lesion counting

After opening along the longitudinal axis, AOM-treated rat colons were fixed in 10% formalin and stained with methylene blue solution, and then subsequently with high iron diamine-Alcian blue procedure (HID-AB) (Caderni *et al.* 2003) for aberrant crypt foci (ACF) and MDF scoring, respectively. Scoring was achieved by one reader who was blinded to the colon sample origin.

Colon histology and immunohistochemistry

A piece of formalin-fixed colon tissue was embedded in paraffin. Paraffin blocks were cut in 4 μm sections that were either stained with hematoxylin/eosin or Alcian blue for mitosis index, microscopic injury score and mucus cell determination, respectively, using light microscopy with 400× magnification.

Hematoxylin/eosin-stained colonic tissue sections were scored by using easily identifiable microscopic criteria, including the extent of cellular infiltration (0–5), declining crypt architecture (crypt damage, 0–5), size and relative extent of ulceration (0–3), goblet cell depletion (absent, 0; present, 1) and absence or presence of edema (0 and 1). The final score ranged from 0 to 15. All slides were analyzed by a single investigator who was blinded to the treatment groups.

For γ-H2AX immunohistochemical staining, paraffin sections were rehydrated and endogenous peroxidase activity was quenched with a 10-min incubation in BLOXALL® solution (Vector Laboratories, USA). After washing slides, antigen retrieval was carried out by heating sections in 0.01 M citrate buffer (pH 6.0) by microwaving (14 min). After incubation in 2.5% normal horse blocking serum (IMMPRESS® HRP Goat Anti-Rabbit IgG Polymer Detection Kit, Vector Laboratories), sections were incubated overnight at 4 °C with rabbit anti-γ-H2AX (1/200, Cell Signaling Technology #9718, USA) diluted in Animal-Free Blocker® solution (Vector Laboratories). After washing, slides were incubated for 30 min with ImmPRESS Polymer Reagent. The DAB (3,3′-diaminobenzidine) substrate kit for peroxidase (ImmPACT®DAB, Vector Laboratories) was used as the chromogen. Sections were then counterstained and mounted. γ-H2AX-positive cells were assessed by counting the positive nuclei in the colonic segment. Positive counts were expressed as a percentage of positive cells per crypt.

To measure RNA/DNA oxidative damage, a mouse monoclonal antibody to 8-OHdG (sc-393871, Santa Cruz Biotechnology, USA) was used at a dilution of 1:500 as the primary antibody with the following adaptations. Antigen recovery was first performed using a low-pressure cooker (15 min, citrate buffer, pH 6), followed by proteinase K for 20 min at 37 °C. After incubation in 2.5% normal horse blocking serum, sections were incubated overnight at 4 °C with mouse anti-8-OHdG diluted in Animal-Free Blocker® solution. After washing, slides were incubated for 30 min with ImmPRESS polymer reagent (IMMPRESS® HRP Horse Anti-Mouse IgG PLUS Polymer Detection Kit, Vector Laboratories). The DAB (3,3′-diaminobenzidine) peroxidase substrate kit

Downloaded from Bioscientifica.com at 07/22/2025 01:00:31PM
via Open Access. This work is licensed under a Creative Commons
Attribution-NonCommercial-NoDerivatives 4.0 International License.
https://creativecommons.org/licenses/by-nc-nd/4.0/

Redox Experimental Medicine (2025) **2025** e250001
https://doi.org/10.1530/REM-25-0001

(ImmPACT®DAB, Vector Laboratories) was used as before. Sections were then counterstained and mounted. The mean number of positive mucosal cells per section is shown.

All slides were analyzed by a single investigator who was blinded to the treatment groups. The histological features shown are representative of all tissue samples studied.

Colon mucosa and liver gene expression assays

Total cellular RNA was extracted with Tri Reagent (Molecular Research Center, USA) from colon scrapped mucosa (proximal part) and liver. Total RNA samples (1 μg) were then reverse-transcribed with the iScript™ Reverse Transcription Supermix (Bio-Rad) for real-time quantitative polymerase chain reaction (qPCR) analyses. The primers for SYBR Green assays are presented in Supplementary Table 1 (see section on Supplementary materials given at the end of the article). Amplifications were performed on a ViiA 7 Real-Time PCR System (Applied Biosystems, USA). The qPCR data were normalized to the level of the RNA polymerase II subunit A (*Polr2a*) messenger RNA (mRNA) and analyzed using the LinRegPCR v.11 software (https://mybiosoftware.com/linregpcr-analysis-quantitative-pcr-data.html).

Urine analyses

Urinary 1,4-dihydroxynonane mercapturic acid (DHN-MA), the major urinary metabolite of HNE and a marker of lipid peroxidation (Peiro *et al.* 2005), was measured as previously described (Guéraud *et al.* 2006) using a homemade anti-DHN-MA polyclonal antibody, Bertin Bioreagent DHN-MA-AChE tracer and Ellman's reagent (Montigny-le-Bretonneux, France). 8-iso-$PGF_{2\alpha}$ and DNA/RNA oxidative damage (high sensitivity) were assayed using Cayman ELISA kits (Bertin Bioreagent), according to the manufacturer's instructions.

Fecal analyses

Fecal waters were prepared from feces collected during 24 h, as described previously (Martin *et al.* 2018). Fecal heme iron was measured as described previously (Pierre *et al.* 2004). Fecal thiobarbituric acid-reactive substances (TBARS) were measured in fecal waters according to Ohkawa *et al.* using tetramethoxypropane (Sigma-Aldrich) as an internal standard and expressed as malondialdehyde equivalents, as recommended by these authors (Ohkawa *et al.* 1979). Fecal HNE was measured as described before by Chevolleau *et al.* (2018). For cytotoxicity and genotoxicity assays, fecal waters were tested on noncancerous mouse colon epithelial cells ('Co cells' (Plaisancié *et al.* 2022)). Those cells are conditionally immortalized normal colonocytes, obtained by mating a heterozygous female 'Immortomouse' with a male C57BL/6J mouse. The cell line was established earlier (Forest *et al.* 2003) and harbors a temperature-sensitive mutation of the simian virus 40 large tumor antigen gene (tsA58) controlled by interferon-γ, which induces the H-2K promoter. Cells were cultured under permissive conditions (33 °C and interferon-γ) and then treated for 24 h with fecal waters at 37 °C (without interferon-γ; nonpermissive conditions) in serum-free DMEM medium in order to avoid any reaction between reactive lipid oxidation products and serum proteins. Fecal water cytotoxicity was assessed using the WST-1 kit and fecal water genotoxicity was measured by 'in-cell western' γ-H2AX assay, as described earlier (Audebert *et al.* 2011), on Co cells. This methodology is detailed in the Supplementary Material (supplementary Material & Methods).

Fecal microbiota analysis

Microbial DNA extraction from frozen anal feces, DNA amplicons (V3–V4 regions of the 16S rRNA gene) and library obtention were performed as previously described (Martin *et al.* 2019). Illumina MiSeq sequencing and validation of its quality were performed at the GeT-PlaGe platform in Toulouse, as previously described (Martin *et al.* 2019). Raw sequences were analyzed through the FROGS v3.1. pipeline (Find Rapidly OTU with Galaxy Solution (Escudié *et al.* 2017)) thanks to Galaxy instance (https://vm-galaxy-prod.toulouse.inrae.fr). Preprocessing, clustering, chimera removal and filtering steps were performed using FROGS recommendations, leading to 562 operational taxonomic units (OTUs). The Silva 138.1_16S database was chosen for the affiliation step and equal multi-hits generated by the Blast+ method may have been assigned manually when justified. An additional prevalence filtering step was applied to remove taxa not seen more than 5 times in at least 5% of the samples, yielding to 527 final OTUs and 3,027,648 valid reads found among the 119 samples (an average of 25,500 reads per sample). Richness and diversity indexes of the bacterial community, as well as ordinations, were computed on rarefied abundances of OTUs agglomerated at the species rank using the Phyloseq package (v 1.34.0) in RStudio software (http://www.rstudio.com; R Development Core Team 2011, McMurdie & Holmes 2012, 2013). Richness (α-diversity) was explored using the Chao-1 index. Weighted UniFrac distance matrices were determined to assess β-diversity, visualized using multidimensional scaling (MDS) and compared using the Adonis test (permuted *P*-value was obtained by performing 9,999 permutations). LDA effect size (linear discriminant analysis) was performed between the three classes using the Kruskal–Wallis test with a one-against-all strategy, and statistically significant features with an absolute logarithmic LDA score higher than 3 were plotted using LEfSe (Segata *et al.* 2011). Some features of interest were agglomerated at the genus level and their relative abundance was preprocessed according to

Downloaded from Bioscientifica.com at 07/22/2025 01:00:31PM
via Open Access. This work is licensed under a Creative Commons
Attribution-NonCommercial-NoDerivatives 4.0 International License.
https://creativecommons.org/licenses/by-nc-nd/4.0/

Redox Experimental Medicine (2025) **2025** e250001
https://doi.org/10.1530/REM-25-0001

Table 1 Serum iron and glutathione-related parameters measured in plasma, colon and liver of rats after the experimental diet period. Serum iron, GSH and GSSG are expressed in μM. Gene expression in the colon and liver is expressed as relative expression to POLR2A. GSH, reduced glutathione; GSSG, oxidized glutathione; GSH/GSSG, ratio of reduced to oxidized glutathione. Data are presented as mean ± SD.

	CON	CFC	Hemin	*P**
Plasma				
GSH	516 ± 148.8	466.3 ± 95.68	265.3 ± 120.9	0.0021
GSSG	141.50 ± 31.19	373.3 ± 58.61	304.4 ± 88.27	< 0.0001
GSH/GSSG	3.64 ± 0.73	1.25 ± 0.26	0.91 ± 0.32	< 0.0001
Colon				
Gclm	7.68 ± 3.49	9.24 ± 5.01	11.07 ± 3.92	0.29
Gclc	0.85 ± 0.33	1.06 ± 0.43	1.36 ± 0.48	0.07
Gsr	0.84 ± 0.40	2.32 ± 0.81	3.07 ± 0.89	< 0.0001
Gss	4.01 ± 1.31	7.92 ± 1.90	8.51 ± 0.96	< 0.0001
Liver				
Gclm	14.18 ± 8.85	12.91 ± 6.97	15.68 ± 8.66	0.80
Gclc	2.63 ± 1.88	2.58 ± 1.96	3.82 ± 2.54	0.44
Gsr	1.36 ± 0.75	1.27 ± 0.64	1.26 ± 0.60	0.65
Gss	3.28 ± 0.67	3.32 ± 0.80	3.44 ± 0.73	0.90

GSH, reduced glutathione; GSSG, oxidized glutathione; GSH/GSSG, ratio of reduced to oxidized glutathione.
*statistical comparison by ANOVA.

the mixMC framework with the offset option and normalized using a centered log-ratio transformation for graph purposes (Lê Cao *et al.* 2016).

Blood/plasma analyses

Plasmatic myeloperoxidase (MPO) and blood glutathione (GSH/GSSG) were assayed as previously described (Stocker *et al.* 2017). Briefly, reduced (GSH) and oxidized glutathione (GSSG) were measured in collected whole blood samples immediately mixed with an equivalent volume of serine borate buffer (pH 8.5) containing L-serine (100 mM), boric acid (80 mM), associated with iodoacetic acid (10 mM), bathophenanthroline disulfonate sodium salt (2 mM) and Na-heparin (2020 USP units). Samples were then plunged rapidly into liquid nitrogen and kept at −80 °C before protein precipitation. HPLC analysis was then performed after the addition of dansyl chloride to form S-carboxymethyl-N-dansyl-GSH and N,N-9-bis-dansyl-GSSG adducts as described earlier. Quantification was based on peak area and relative to standards from a calibration curve obtained with commercial GSH and GSSG. Data were expressed (in μM) as means from n = 8 independent blood samples in each group, analyzed in triplicate. C-reactive protein was measured in serum using a C-reactive protein (PTX1) Rat ELISA kit (Abcam, France).

Statistical analysis

All data, except for microbiota analyses, were analyzed using GraphPad Prism Software (https://www.graphpad.com/) by one-way ANOVA followed by Tukey's multiple comparison test, after log transformation in case of variance inequality or the Kruskal–Wallis test when data did not meet normality requirements for ANOVA. Outliers were removed from analyses after a ROUT test. A P-value <0.05 was considered significant. Results are presented as mean ± SD.

Results

Zootechnic parameters

Hemin and ferric citrate diets did not modify rat weight during the experiment, when compared to the control diet. At the end of the experimental diets, rat weight was 266 ± 20 g for the control (CON) group, 267 ± 19 g for the ferric citrate (CFC) group and 266 ± 22 g for the hemin group.

Hemin diet and more modestly ferric citrate diet, increased lipid peroxidation biomarkers

We found around 70 times more heme iron in the fecal waters of hemin-fed rats compared to the other groups (556 ± 118 μM for the hemin group, vs 7 ± 3 and 8 ± 12 μM for the CON and CFC diets, respectively). Yet, no differences were observed between the groups for serum iron (Table 1). As heme-induced luminal lipid peroxidation was our hypothesis to explain the heme iron putative effect, we checked that fecal and urinary lipid peroxidation markers were increased by the hemin diet. Indeed, the hemin diet dramatically increased lipid peroxidation biomarkers in fecal water and urine, while the ferric citrate diet increased those biomarkers to a much lesser extent (Fig. 1A and supplementary Fig. 1A). At the end of the experimental diets, fecal TBARS of hemin-diet-fed rats were more than 4 times higher than those of the two other groups, while fecal HNE was increased by ten times and almost by seven times by the hemin diet

Downloaded from Bioscientifica.com at 07/22/2025 01:00:31PM
via Open Access. This work is licensed under a Creative Commons
Attribution-NonCommercial-NoDerivatives 4.0 International License.
https://creativecommons.org/licenses/by-nc-nd/4.0/

Redox Experimental Medicine (2025) **2025** e250001
https://doi.org/10.1530/REM-25-0001

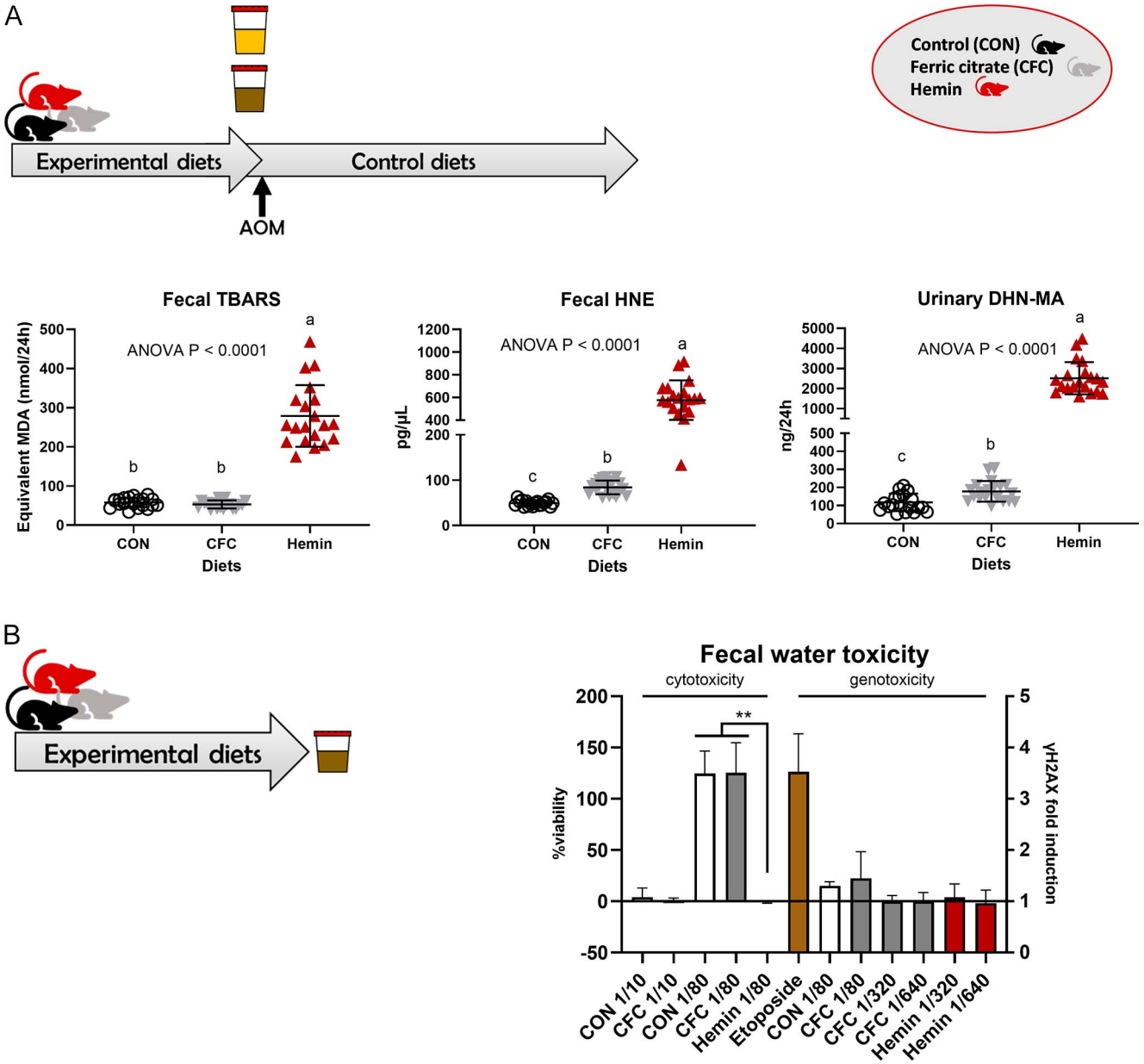

Figure 1

(A) Fecal water and urinary lipid peroxidation biomarkers. Samples were assayed at the end of the experimental diet period (2 weeks) in AOM-treated rats. AOM, azoxymethane. Data are represented as mean ± SD. *P* value for ANOVA is indicated on the graphs. Groups displaying different letters indicate that the *P* value calculated for the pairwise comparison of these groups is smaller than the alpha level ($P < 0.05$) and considered statistically different. (B) Fecal water cytotoxicity (left) and genotoxicity (right) at various dilutions at the end of the experimental diet period on Co cells. Etoposide is used as a positive control. Data are represented as mean ± SD. ** means significant difference with $P < 0.01$.

when compared to the control and the ferric citrate diets, respectively.

The increase in urinary DHN-MA, the major urinary metabolite of HNE, was even more important, with a 21- and a 14-fold increase with the hemin diet when compared to the control or the ferric citrate diet, respectively (all ANOVA $P < 0.0001$) (Fig. 1A).

Hemin diet, but not ferric citrate diet, induced a cytotoxic environment for colon epithelial cells

Fecal waters from the hemin-diet-fed rats were much more cytotoxic to murine colon immortalized epithelial cells (Co cells) at a dilution of 1/80, while fecal waters from the control or ferric citrate diets had no deleterious effect

Downloaded from Bioscientifica.com at 07/22/2025 01:00:31PM
via Open Access. This work is licensed under a Creative Commons
Attribution-NonCommercial-NoDerivatives 4.0 International License.
https://creativecommons.org/licenses/by-nc-nd/4.0/

Redox Experimental Medicine (2025) **2025** e250001
https://doi.org/10.1530/REM-25-0001

at this concentration (Fig. 1B). Hemin-diet fecal waters were not genotoxic to those immortalized colon cells at a dilution of 1/640, a high dilution necessary to avoid any cytotoxic effect that would distort the genotoxic effect assay.

Hemin and ferric citrate diets increased lipid peroxidation/antioxidant defenses in rat colon mucosa

The hemin diet, but also the ferric citrate diet, modulated the expression of genes usually modified by heme iron in the colon at the end of the experimental diet period. The hemin diet concomitantly induced the expression of *Nrf2* (+67% compared to the control diet) and of its repressor *Keap1* (3.4-fold increase when compared to control diet). *Nrf2*-driven canonical gene expression (*Hmox1* and *Nqo1*) was also increased by hemin (2.4 and 6 times, respectively), but also by ferric citrate (1.8 and 3.2 times, respectively), while *Bach1* expression was decreased (by 38 and 28% by the hemin and ferric citrate diets, respectively) (Fig. 2A and Supplementary Fig. 1B). All these genes were supposed to be modulated by heme iron. In fact, except for *Nrf2* expression, all effects were statistically significant with both ferric citrate and heme iron when compared to the control, although the hemin effect tended to be more important than the ferric citrate one, with a significant difference between those two diets for *Hmox1*. Most of HNE-metabolizing enzyme gene expressions (*Aldh2*, *Ptgr1*, *Akr1b10* and *Akr1b7*), were significantly increased by hemin and ferric citrate in diets, while *Akr1b8* and *Aldh3a2* were only increased by the hemin diet and *Gsta4* was unaffected (Fig. 2B and Supplementary Fig. 1B). For glutathione-related enzyme gene expressions, *Gsr* and *Gss* were also significantly increased by both iron-supplemented diets, and *Gclc* followed a similar trend, although not statistically significant (P = 0.07) (Table 1). Glutathione-related enzyme gene expressions were not affected by the different diets in the rat liver (Table 1).

Hemin diet, but not ferric citrate diet, given before the chemical initiation of CRC, increased the number of big ACF and of mucin depleted foci in rat colons

The hemin diet, but not the ferric citrate one, given before azoxymethane initiation increased the two types of preneoplastic lesions in the colon of rats, when compared to the control diet (Fig. 3A and B). The hemin diet increased the size of ACF by 10% (ANOVA P = 0.0001) and the number of ACF with more than seven crypts by 90% (ANOVA P < 0.0001) when compared to the ferric citrate diet, although the total number of ACF remained unchanged. The number of MDF increased by 114% (ANOVA P = 0.0012) when compared to the ferric citrate diet, and this increase was even more important in the distal part of the colon, with a 168% increase (ANOVA P < 0.0001). Just after the experimental diet period, the hemin diet increased the hematoxylin-based mitosis index, a measure of cellular proliferation, in the colon of rats by 155% (ANOVA P = 0.024), when compared to the control diet (Fig. 3C), while this effect was no longer observed at the end of the protocol, with even a trend toward a decrease (−27%) observed in the hemin group (ANOVA P = 0.06). The hemin diet reduced the number of mucus (goblet) cells in the rat colon by 43% (ANOVA P = 0.0004). The ferric citrate diet had an intermediate, but not significant effect (Fig. 3D), while this effect is no longer observed at the end of the protocol, with even an increased number of mucus cells (+23%; ANOVA P = 0.0137) with the ferric citrate diet when compared to the control one, and a similar trend for the hemin diet. However, it is important to note that, due to preneoplastic lesion counting, colon tissue samples were not taken from the same location at the end of the diet period or at the end of the protocol, i.e. the median part and the very proximal part, respectively.

Hemin diet had diverse effects on two genotoxicity biomarkers in the colon mucosa of rats, together with increased systemic oxidative stress

The hemin diet induced significantly more oxidized RNA/DNA bases, measured as 8-OHdG by immunohistochemistry, than the control diet (+77%) but also than the ferric citrate diet (+120%), in the colon of the rats, at the end of the experimental diet period (Fig. 4A).

Unexpectedly, both hemin and ferric citrate diets provoked an important decrease in γ-H2AX, a marker for DNA double-strand breaks measured by immunohistochemistry, in the colon of rats (Fig. 4B) (more than a three-fold decrease, ANOVA P = 0.0001) at the end of the diet period. This decreasing effect remained important at the end of the protocol, especially for the hemin diet (ANOVA P < 0.0001) (Supplementary Fig. 1C). A similar trend has been observed using an in-cell western methodology, although far less pronounced (Supplementary Fig. 1C), while with the same methodology a decrease in phospho-histone 3 (p-H3), a mitosis biomarker, was observed (ANOVA P = 0.03), reinforcing the result obtained with the hematoxylin-based mitosis index at the end of the protocol (Supplementary Fig. 1C).

At the same time, both diets had an important effect on blood reduced and oxidized glutathione (Table 1), with the ratio of reduced to oxidized glutathione (GSH/GSSG) divided by four and almost by three

Downloaded from Bioscientifica.com at 07/22/2025 01:00:31PM
via Open Access. This work is licensed under a Creative Commons
Attribution-NonCommercial-NoDerivatives 4.0 International License.
https://creativecommons.org/licenses/by-nc-nd/4.0/

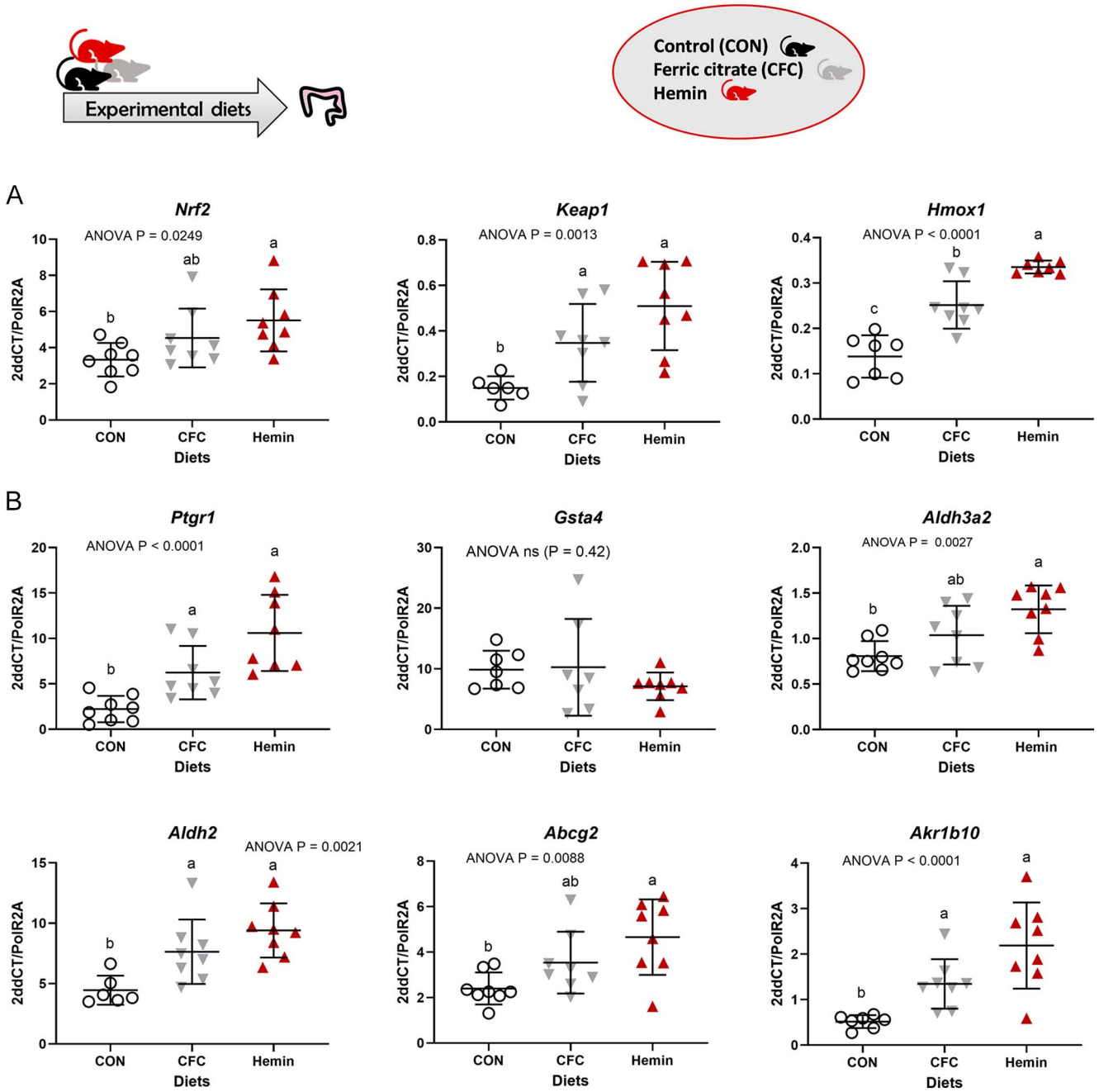

Figure 2

(A and B) Gene expression in rat colon mucosa at the end of the experimental diet period, in rats euthanized before AOM treatment. Data are represented as mean ± SD. *P* value for ANOVA is indicated on the graphs. Groups displaying different letters indicate that the *P* value calculated for the pairwise comparison of these groups is smaller than the alpha level ($P < 0.05$) and considered statistically different.

with hemin and ferric citrate diets, respectively (ANOVA $P < 0.0001$). Only the hemin diet induced more than two-fold increase in urinary 8-isoprostane (ANOVA $P < 0.0001$) at the end of the diet period (Fig. 4C). Both biomarkers indicate systemic oxidative stress. The hemin diet increased urinary excretion of oxidized DNA bases, measured as the sum of 8OH-G, 8OH-dG and 8OH-guanine, when compared to the ferric citrate diet (+46%, Kruskal–Wallis $P = 0.04$) at the end of the experimental diets, revealing that rats were undergoing an oxidative genotoxic process, reinforcing the results in the colon by immunohistochemistry (Fig. 4C).

Downloaded from Bioscientifica.com at 07/22/2025 01:00:31PM
via Open Access. This work is licensed under a Creative Commons
Attribution-NonCommercial-NoDerivatives 4.0 International License.
https://creativecommons.org/licenses/by-nc-nd/4.0/

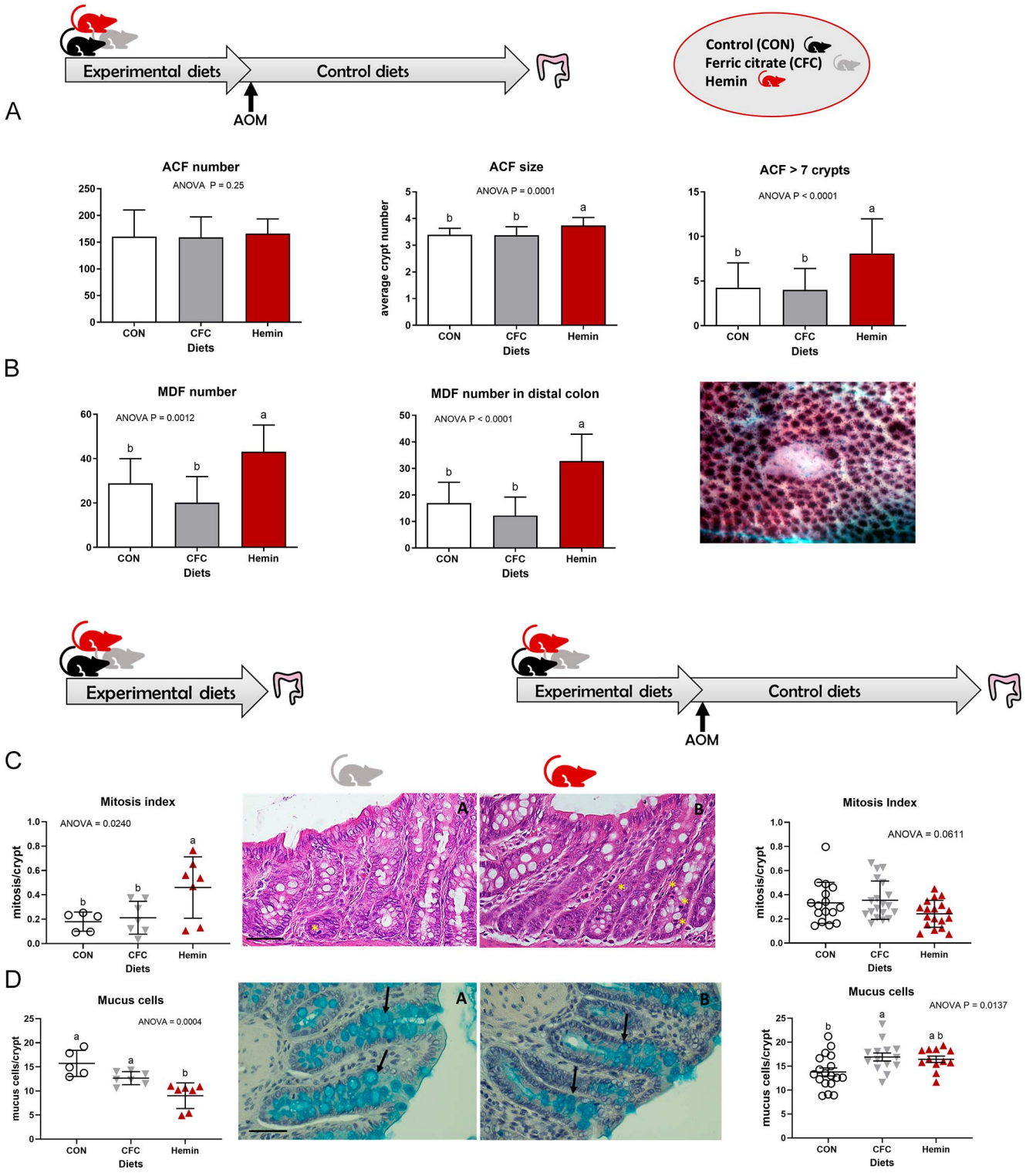

Figure 3

(A) Scoring of ACF and aberrant foci size in rat colons in AOM-treated rats. (B) Scoring of MDF in the whole colon and in the distal part in AOM-treated rats, representative picture of an MDF after HI-DAB staining of mucus in crypts. (C) Hematoxylin-eosin scoring of mitosis/crypt in the rat colon at the end of the diet period (left) and in the AOM-treated rat colons (right), representative pictures (×40) in CFC (left (A)) and hemin (right (B)) rat colons (median part) at the end of the diet period, scale bar: 50 μm, * indicates example of positive cells and (D) Histochemical (Alcian blue) scoring of mucus cells/crypt in the rat colon at the end of the diet period (left) and in the AOM-treated rat colons (right), representative pictures in CFC (left (A)) and hemin (right (B)) rat colons (median part) at the end of the diet period, scale bar: 50 μm, arrows indicate fewer mucus cells in the hemin-fed rat group. AOM, azoxymethane. Data are represented as mean ± SD. *P* value for ANOVA is indicated on the graphs. Groups displaying different letters indicate that the *P* value calculated for the pairwise comparison of these groups is smaller than the alpha level ($P < 0.05$), and considered statistically different.

Downloaded from Bioscientifica.com at 07/22/2025 01:00:31PM
via Open Access. This work is licensed under a Creative Commons
Attribution-NonCommercial-NoDerivatives 4.0 International License.
https://creativecommons.org/licenses/by-nc-nd/4.0/

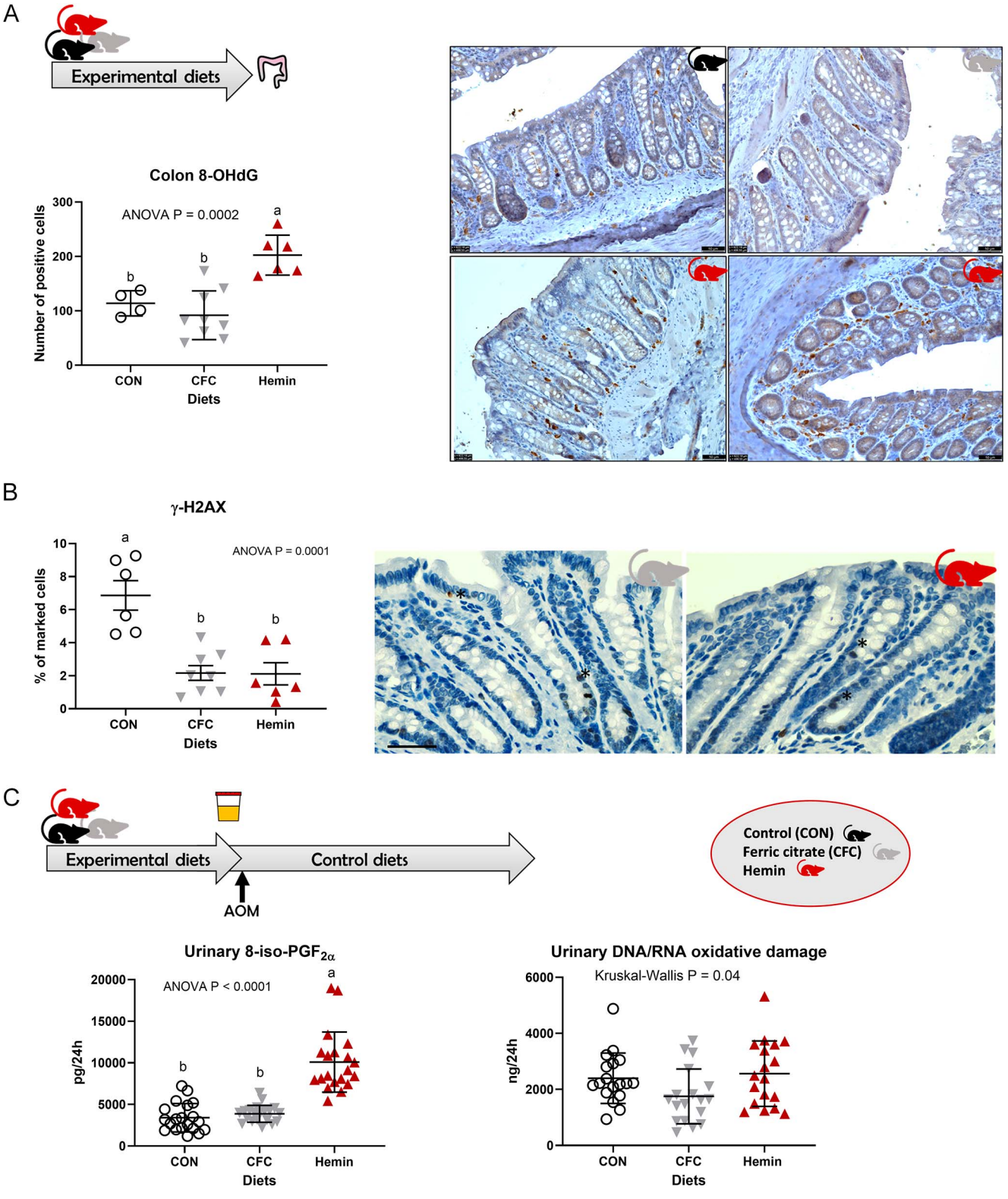

Figure 4

(A) Representative pictures of oxidative damage in colonic mucosa detected by 8-OHdG immunohistochemistry at the end of the experimental diet period. Low reactivity in colon tissue of CON (up/left) and CFC (up/right). High 8-OHdG reactivity in the colon (median part) of hemin-fed rats (longitudinal (down/left)) and transverse (down/right) sections of crypts). Positive cells are mainly observed in the lamina propria. (IHC, ×40). (B) Immunohistochemical staining of γ-H2AX (diaminobenzidine (DAB), brown) in the rat colon at the end of the diet period, representative pictures in CFC (left) and hemin

Downloaded from Bioscientifica.com at 07/22/2025 01:00:31PM
via Open Access. This work is licensed under a Creative Commons
Attribution-NonCommercial-NoDerivatives 4.0 International License.
https://creativecommons.org/licenses/by-nc-nd/4.0/

Figure 4 (Continued)

(right) rat colons (median part) at the end of the diet period, scale bar: 50 μm, * indicates examples of positive cells. (C) Urinary oxidative stress and oxidative genotoxicity biomarkers. Samples were assayed at the end of the experimental diet period. AOM, azoxymethane. Data are represented as mean ± SD. *P* value for ANOVA is indicated on the graphs. Groups displaying different letters indicate that the *P* value calculated for the pairwise comparison of these groups is smaller than the alpha level ($P < 0.05$), and considered statistically different.

Hemin and ferric citrate diets had various effects on colon and systemic inflammation biomarkers

The hemin diet significantly reduced colon length at the end of the protocol in the AOM-treated rats (19.53 cm ± 1.55; 19.93 cm ± 0.92; 18.83 cm ± 1.39 for CON, CFC and hemin diets, respectively, ANOVA $P = 0.048$). Both hemin and ferric citrate diets had an inducing effect on plasma myeloperoxidase (+47 and 59%, respectively, ANOVA $P < 0.0001$) but not on C-reactive protein (Fig. 5A), measured at the end of the diet period. At the end of the diet period, a trend toward an increase, but not statistically significant, in the microscopic injury score, which includes cellular infiltration (ANOVA $P = 0.19$) and in *Cox2* expression (ANOVA $P = 0.111$) could be observed (Fig. 5B) with the hemin diet. A significant decrease in colon IL1-β was observed with this diet compared to the other two diets (ANOVA $P = 0.0015$), while colon IL-6 and TNFα were not significantly modified by the diets, with a very high variability observed in the hemin diet group (results not shown).

Hemin diet, but not ferric citrate one, deeply modified rat fecal microbiota; this modification is no longer observed when this diet was stopped for 8 weeks

The hemin diet, but not the ferric citrate one, modified fecal microbiota diversity (Fig. 6A and supplementary Fig. 2) after 12 days of diet (week 02).

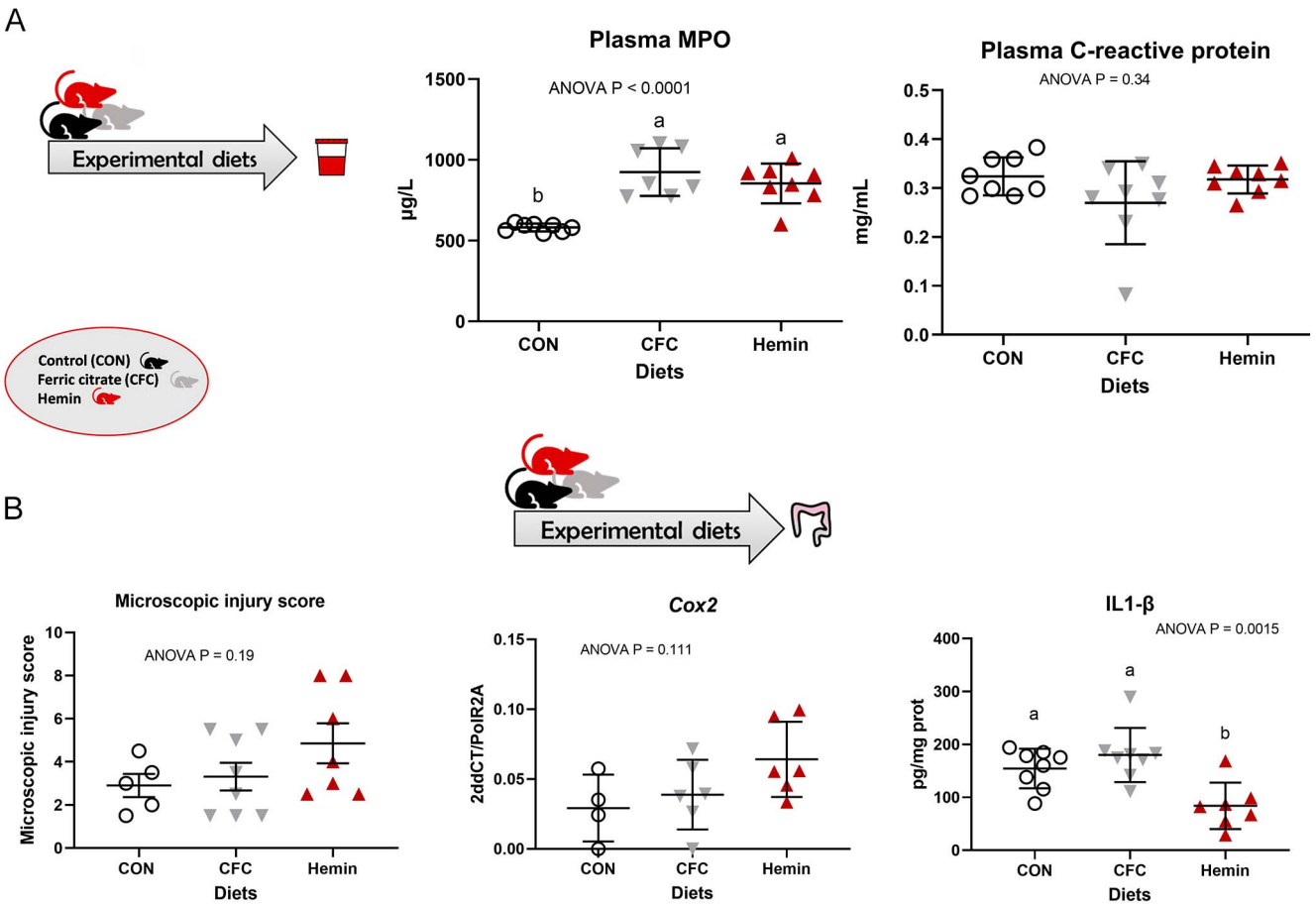

Figure 5

(A) Systemic plasma inflammation biomarkers at the end of the experimental diet period. MPO, myeloperoxidase; (B) inflammation-related biomarkers in the colon of rats at the end of the diet period; left: microscopic injury score; middle: Cox2 gene expression; right: IL1-β protein concentration. Data are represented as mean ± SD. *P* value for ANOVA is indicated on the graphs. Groups displaying different letters indicate that the *P* value calculated for the pairwise comparison of these groups is smaller than the alpha level ($P < 0.05$), and considered statistically different.

Downloaded from Bioscientifica.com at 07/22/2025 01:00:31PM
Open Access. This work is licensed under a Creative Commons Attribution-NonCommercial-NoDerivatives 4.0 International License.
https://creativecommons.org/licenses/by-nc-nd/4.0/

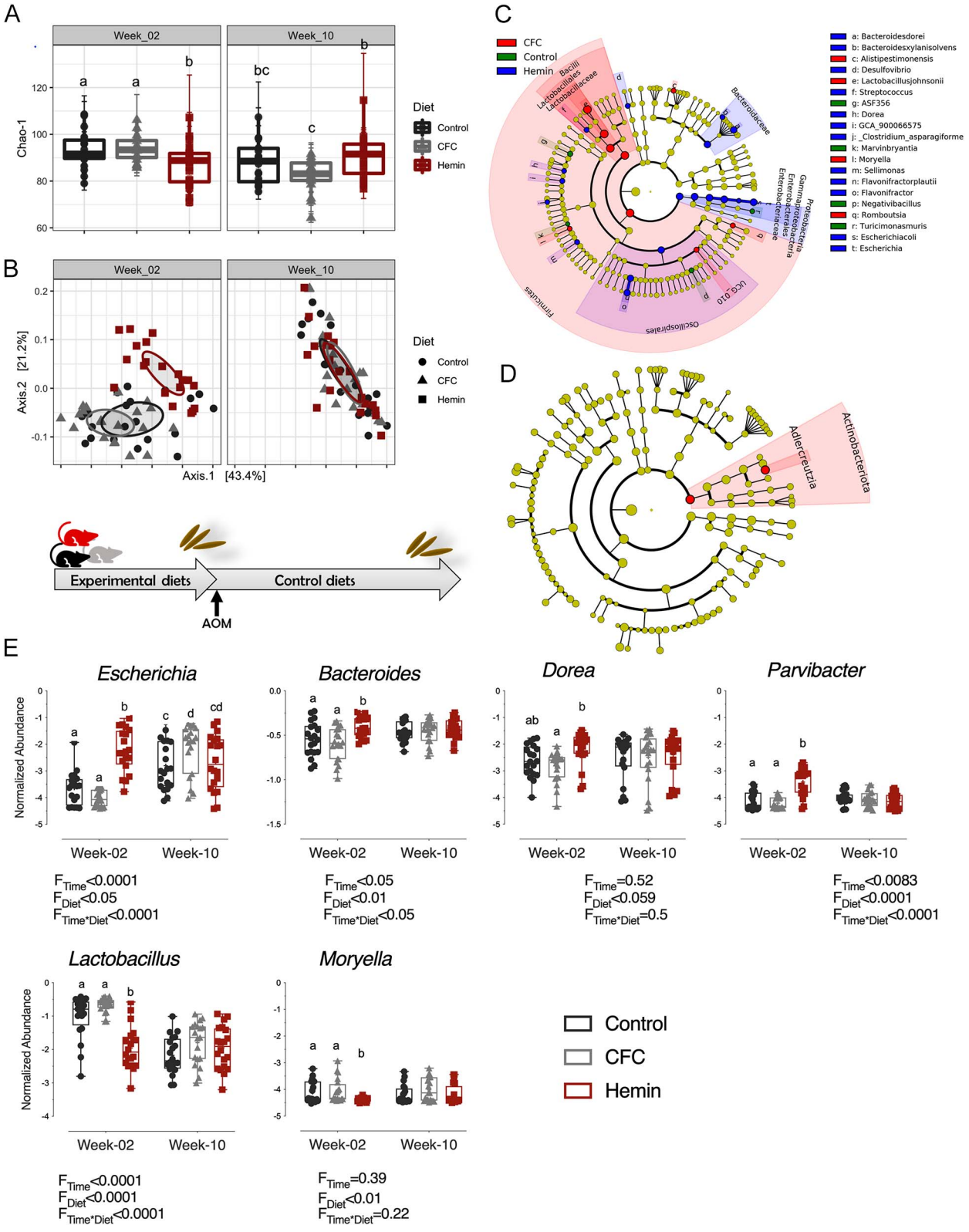

Figure 6

16S rRNA amplicons sequencing analysis of the rat fecal microbiota. Fecal samples were collected at week 02 (at the end of the experimental diet period) and at week 10, after 8 weeks of control or CFC diet, in AOM-treated rats. A total of 120 fecal samples were collected. AOM, azoxymethane. (A) Alpha diversity analyzed by Chao-1 index. (B) MDS results based on weighted UniFrac distances. (C) Distinctive fecal microbiota composition according to diet

Downloaded from Bioscientifica.com at 07/22/2025 01:00:31PM
via Open Access. This work is licensed under a Creative Commons
Attribution-NonCommercial-NoDerivatives 4.0 International License.
https://creativecommons.org/licenses/by-nc-nd/4.0/

Figure 6 (Continued)

using LEfSe analysis at week 02 ($P < 0.01$). (D) Distinctive fecal microbiota composition according to diet using LEfSe analysis at week 10 ($P < 0.05$). Taxa enriched in the fecal microbiota of rats fed the control, CFC or hemin diet are represented in green, red and blue, respectively. (E) Normalized abundance of some relevant features at the genus level as box plots. Different letters mean that groups are significantly different with two-factor analysis (mixed-effect, type III) followed by Holm-Šídák's multiple comparisons test at week 02 or 10. n = 19–20.

This modification is no longer observed at week 10, after 8 weeks of control or CFC diet. This diet modified alpha diversity, as evidenced by a significant decrease in richness (Chao-1), but this index was normalized to the control group once the hemin diet was stopped (two-way factor analysis (type III): F_{Diet} = 0.399, F_{Time} = 0.00395, $F_{DietxTime}$ = 0.000317, Holm-Šídák's multiple comparisons test Week-02: control vs CFC 0.8755, control vs hemin 0.0287, CFC vs hemin: 0.0281; Week-10: Control vs CFC 0.842; Control vs Hemin 0.2741; CFC vs Hemin: 0.0066). Beta-diversity assessment using weighted UniFrac distances revealed dietary heme iron-associated changes in fecal bacterial ecology: hemin-fed rats at week 02 clustered separately from control- and CFC-fed rats, whereas they all clustered together at week 10 (Fig. 6B), suggesting a common evolution within bacterial communities over time in response to control diets (Adonis factor analysis: $F_{Diet} < 0.0001$, $F_{Time} < 0.0001$, $F_{DietxTime}$ = 0.0001). LEfSe results showed that microbiota composition was also highly dependent on the form of iron added to the diet: in response to the hemin diet (week02), *Enterobacteriaceae* such as *Escherichia coli* within *Proteobacteria,* several species within *Bacteroidaceae,* and some members belonging to *Firmicutes* such as *Dorea* and *Parvibacter*, were enriched and associated with a decrease in *Firmicutes*, mainly due to *Lactobacillaceae* and, to a lesser extent, to *Moryella.* ($P < 0.01$ Fig. 6C and E). At week 10, none of the above taxa revealed differential abundance. Only *Adlercreutzia* at the genus level within *Actinobacteriota* was enriched in CFC-fed rats at $P < 0.05$ (Fig. 6D and E).

Discussion

In our previous studies, we showed that dietary heme iron, given as hemin (purified heme molecule), hemoglobin (hemoprotein), red meat or black pudding (hemoglobin-rich specialty), had a promoting effect in AOM-initiated CRC model animals or in Min mice (Pierre *et al.* 2003, 2004). AOM is a colonotropic alkylating agent. For these CRC-promotion studies, dietary heme iron was given after the initiating event, namely AOM intraperitoneal injection. In the present study, the same dietary dosage of hemin was used but for a short 2-week period, just before the initiating event, in order to determine if this compound could also have a co-initiating effect on CRC development. The dietary concentration of hemin used is representative of human dietary habits of red meat 'big eaters'. This choice was dictated by the fact that it is precisely these heavy red meat eaters who are most at risk of developing CRC (Vieira *et al.* 2017). According to Lombardi-Boccia *et al.* (2002), the iron content of cooked beef red meat varies, in its heminic form, between 1.89 and 3.14 mg per 100 g of fresh meat. Considering an average dry weight of cooked beef meat of 35% (Ciqual, ANSES, https://ciqual.anses.fr/), it varies from 5.4 to 8.97 mg per 100 g of dry weight. For the present study, we used semi-synthetic dry AIN-76-type diets with 0.094% hemin, which provided 8 mg of iron in its heminic form per 100 g of diet. This hemin concentration has been used in previous studies on the promoting effect of heme iron on CRC by our group and similar concentrations by others (Sesink *et al.* 1999, 2000, 2001). In the present study, the ferric citrate control group (CFC) diet contained the same amount of iron but in a non-heminic form. The presence of two control groups (with or without a supplement in ferric citrate, namely CFC and CON) allowed to determine if the observed effects were due to the amount of iron or its form (heminic or non-heminic).

AOM- (or dimethylhydrazine-) initiated F344 rats are widely used animal models to study the promoting or preventive effects of compounds on CRC development, with the compounds given after the initiating event (Corpet & Taché 2002). Testing compounds as co-initiators of AOM by giving them just before the AOM treatment is not a so widespread protocol. Nevertheless, other groups used such an experimental design to analyze the co-initiating effect of compounds given before AOM (Poulsen *et al.* 2001, Liu & Xu 2008) or, on the contrary, their protective effects (Kim *et al.* 2001). With such a 'co-initiation' experimental protocol, we showed in the present study that iron in its heminic form, but not in its ferric citrate form, increased the number of MDF and the size of ACF. ACF were first evidenced by Bird's group as preneoplastic lesions that could represent appropriate predictive markers of colon neoplastic events in murine models of CRC (Bird 1987, Tudek *et al.* 1989). Since then, those biomarkers have been widely used in CRC studies to evaluate promotive or protective effects of foods and drugs in preclinical models and in human beings. However, the predictive potential of such premalignant lesions has been a matter of debate (Takayama *et al.* 1998, Lance & Hamilton 2008, Stevens *et al.* 2008), but finally seems to be useful for studies dealing with CRC prevention or promotion (Clapper *et al.* 2020). On the other side, MDF are preneoplastic lesions evidenced in the colon of AOM-treated rats by Caderni's group (Caderni *et al.* 2003, Femia *et al.* 2004). They show frequent Apc gene, beta-catenin gene mutations and an altered beta-catenin cellular localization, demonstrating Wnt signaling activation, a hallmark of colorectal carcinogenesis (Femia *et al.* 2005, 2007).

Downloaded from Bioscientifica.com at 07/22/2025 01:00:31PM
via Open Access. This work is licensed under a Creative Commons
Attribution-NonCommercial-NoDerivatives 4.0 International License.
https://creativecommons.org/licenses/by-nc-nd/4.0/

Redox Experimental Medicine (2025) **2025** e250001
https://doi.org/10.1530/REM-25-0001

Those preneoplastic lesions are then believed to be cancer precursors and pertinent markers in short-term studies on carcinogenesis in animal models (Cui *et al.* 2012), in which, in order to reduce animal suffering and protocol duration, experiments are stopped before tumor emergence. Moreover, these lesions were also identified in human colons of familial adenomatous polyposis and sporadic CRC subjects (Femia *et al.* 2008). The fact that we observed, in the present study, an increasing effect of the hemin diet on both preneoplastic markers, particularly on MDF number, strengthens the conclusion that heme iron co-initiated CRC in a preclinical model.

The heme iron diet, given for 2 weeks before the initiating event, has resulted in a huge increase in luminal lipid peroxidation, confirming the results obtained in the previous studies of our group [9, 10 and 23], as shown by the fecal TBARS (global lipid peroxidation) and HNE (specific for omega-6 fatty acids oxidation) assays. Moreover, the urinary excretion of DHN-MA, the major urinary metabolite of HNE (Fig. 1A and supplementary Fig. 1A), whose excretion is 25 times higher with the hemin diet, indicated that massive amounts of HNE were absorbed. The ferric citrate diet also induced the production of HNE and its excretion into urine, but modestly compared to the heme iron one, indicating that inorganic iron might also catalyze dietary fatty acid oxidation. This luminal important lipid peroxidation, rather than hemin itself, induced a high cytotoxicity of fecal water, the bioavailable part of feces. Indeed, in a previous study, we reported a cytotoxic effect of hemin only if peroxidation-prone polyunsaturated fatty acids were concomitantly present in the diet, indicating this indirect effect of hemin through lipid peroxidation products, such as the cytotoxic HNE (Pierre *et al.* 2007, Guéraud *et al.* 2015). This increase in lipid peroxidation was accompanied by the activation of the Nrf2/Keap1 pathway, namely the expression of this transcription factor and its target genes (*Hmox1* and *Nqo1*), in colon mucosa, and by a clear decrease in *Bach1* expression by both iron-supplemented diets (Fig. 2A and supplementary Fig. 1B). This effect on *Bach1* expression is noteworthy, given the implication of Bach1 in cancer, considered as deleterious in some studies (Lee *et al.* 2019, Wiel *et al.* 2019), but also as a promoter of ferroptosis, a cell death type related to iron and lipid peroxidation (Nishizawa *et al.* 2023). In the same way, most of the expression of enzymes that are involved in HNE detoxification were also induced by both iron-supplemented diets (Fig. 2B and supplementary Fig. 1B). Of particular interest is PTGR1, an enzyme first known to be involved in prostaglandin metabolization but also reported to participate in HNE biotransformation (Dick *et al.* 2001). By catalyzing the reduction of the alpha-beta double bond of HNE, and possibly other related alkenals, this enzyme prevents the Michael addition of those soft electrophilic compounds to cellular proteins and subsequently decreases their biological/toxic action. This protein has been reported to be increased in hepatocellular carcinoma, probably due to a concomitant activation of the Nrf2/Keap1 pathway (Sánchez-Rodríguez *et al.* 2017), as observed in the present study. The expression of other HNE-metabolizing enzymes, except *Gsta4*, was induced by iron-supplemented diets, with no statistically significant difference between ferric citrate and heme iron, although showing an increasing trend with iron in its heminic form compared to ferric citrate. All of these enzymes were reported to be Nrf2 target genes. This antioxidant pathway was reported to act as a double-edged sword, allowing normal cells to resist oxidative events but at the same time giving a selective advantage to preneoplastic cells because of their sustained overactivation of this pathway (Menegon *et al.* 2016). This activation of the Nrf2/Keap1 pathway may have not been sufficient to detoxify the huge amounts of HNE and related lipid peroxidation products reaching colon epithelial cells, letting these compounds exert their proliferative, cytotoxic and genotoxic effects when animals were fed the hemin diet. The decrease in mucus-producing cells observed with the hemin diet could also contribute to this massive absorption of lipid peroxidation products by reducing the barrier effect (Fig. 3D). This result is in agreement with a previous report of Ijssennagger *et al.* that demonstrated a decrease in *Muc2* mucin expression in mice fed a heme-rich diet (Ijssennagger *et al.* 2015). Other authors reported a thinner inner mucus layer in humans with high red meat intake (Jawhara *et al.* 2020). This decrease in the population of mucus cells could contribute to the co-initiating effect of hemin. Indeed, mucus cells are the only cells responsible for the production of the secreted mucin MUC2, the main constituent of the colonic mucus gel. The mucus layer is a crucial defensive barrier that lubricates the intestinal surface, limits the passage of toxic molecules, enteric pathogens and microbiota. The major importance of goblet cells and MUC2 mucin has been clearly demonstrated by the development of spontaneous colitis and intestinal tumors in *Muc2* knockout mice (Van der Sluis *et al.* 2006). Glutathione is a major scavenger of HNE and related compounds. Although the expression of glutathione synthase and glutathione reductase is increased with both iron-rich diets in colon mucosa, the GSH/GSSG ratio is decreased in the plasma of rats fed those diets, with no major difference between the two diets (Table 1), indicating that this pathway was unable to cope with the excess peroxidation associated with those diets.

This excess luminal peroxidation may have consequences locally on colon mucosa, which could explain the increase in preneoplastic lesions that were observed. Indeed, HNE was reported to be involved in most cellular signaling pathways, leading, depending on its concentration and on the cell type involved, to major events concerning cellular processes and fate (Guéraud *et al.* 2010, Csala *et al.* 2015, Guéraud 2017). In the present study, proliferation was

Downloaded from Bioscientifica.com at 07/22/2025 01:00:31PM
via Open Access. This work is licensed under a Creative Commons
Attribution-NonCommercial-NoDerivatives 4.0 International License.
https://creativecommons.org/licenses/by-nc-nd/4.0/

Redox Experimental Medicine (2025) **2025** e250001
https://doi.org/10.1530/REM-25-0001

increased by the hemin diet in the colon, as measured by the mitosis index (Fig. 3C). This hyperproliferative effect of a hemin diet has been reported before by Van der Meer's group, using various biomarkers (Sesink *et al.* 1999, 2000, de Vogel *et al.* 2008), and by Seiwert *et al.* (2021), using the proliferating cell nuclear antigen marker and mitotic index. The heme iron diet-induced hyperproliferation could be explained by a disruption of the regulation of the Wnt/β-catenin signaling pathway that plays a major role in the maintenance and proliferation of intestinal stem cells. Indeed, Ijssennagger *et al.* (2012) showed that heme downregulates proliferation feedback signals such as the Wnt inhibitor factor 1 from surface cells to crypt cells. This effect could be related to the increase in preneoplastic lesions, but the link with the increased exposure to HNE in the colon lumen is not so obvious, as this compound was reported to have various effects on the proliferative activity of cells, depending mostly on its concentration, cell type and biotransformation capacity (Csala *et al.* 2015). It is noteworthy that this proliferative effect of the hemin diet is no longer observed, and even with a tendency to decrease, in the rats at the end of the protocol, when the experimental diets were stopped 2 months before the colons were sampled for analysis.

The hemin diet has been previously reported to be genotoxic (Martin *et al.* 2019), as HNE and related compounds (Eckl *et al.* 1993, Eckl 2003). In the present study, we measured the amount of two genotoxicity markers by immunohistochemistry in the colon sections of rats. The first one, 8-OHdG, is an indicator of oxidative RNA/DNA damage. We observed a clear increase in 8-OHdG, roughly doubled with the hemin diet at the end of the experimental diet period when compared to the CON or ferric citrate diet. This result was expected due to the oxidative processes induced by heme iron and confirms the genotoxic effect of the hemin diet observed previously by our group using the Comet assay (Martin *et al.* 2019). Surprisingly, 8-OHdG staining was almost exclusively observed in the *lamina propria* and not in the epithelial cells. This could be explained by the higher sensitivity to HNE of fibroblasts compared to colon epithelial cells, as described by Eckl & Bresgen (2017). In a previous work on CRC-initiating properties of HNE *in vitro*, our group reported that HNE-treated fibroblasts increased the ability of colonocytes to grow in anchorage-independent conditions, a characteristic of transformed cells, using co-culture in a soft agar assay (Dupuy *et al.* 2024). Studies have shown that oxidative stress promotes the differentiation of different cell populations into activated fibroblasts (or myofibroblasts), which play a major role in tumorigenesis processes (Dang *et al.* 2021, Li *et al.* 2023). The second one, γ-H2AX, is a marker of DNA double-strand breaks, involved in recruiting DNA repair enzymes. Unexpectedly, colon sections from hemin-fed rats contained significantly less γ-H2AX-marked cells than those from control-fed diet. Ferric citrate diet-fed rats showed an intermediate status (Fig. 5A). This surprising result was not limited to the experimental diet period but remained even stronger at the end of the protocol. This was confirmed by γ-H2AX protein quantification by an adapted technique of 'in-cell western' in colon tissue, in which a decreasing trend was also observed (supplementary Fig. 1C). In the same way, no increase in fecal water genotoxicity to epithelial colon cells was observed using the same marker (Fig. 1B). However, it is important to note that, due to their very extensive cytotoxicity, fecal waters from hemin-fed rats were diluted by a large factor to be used for the genotoxicity assay. This 'protective' effect of hemin toward colon genotoxicity measured by a DNA double-strand break marker could be explained by the set of antioxidant defenses induced concomitantly and by an induction of DNA repair capacities, as reported by some authors (Cabelof *et al.* 2002, Jayakumar *et al.* 2015). Alternatively, a protective effect of hemin administered by other routes has been reported and attributed to *Hmox1* induction, leading to the production of hemin antioxidant metabolites biliverdin and bilirubin (Guan *et al.* 2009, Worou *et al.* 2011). The results we report in the present study are not in accordance with previous observation done by our group and others on γ-H2AX. Bastide *et al.* (2015) reported an increase of this marker by immunohistochemistry in the small intestine of hemoglobin-fed *Min* mice for 49 days, and Seiwert *et al.* (2021) reported a clear increase of this marker in the colon of hemin-fed mice, but with six times less hemin in the diet than in the present study and with the diet given for 162 days instead of 2 weeks in the present study. These discrepancies could then be due to different heme iron administration conditions to the animals (hemin vs hemoglobin; different dosage; diet preparation; experimental diet duration) and to the different animal models used (rat vs mouse), with differences in antioxidant defenses.

At the same time, we observed a moderate but significant increase in the urinary excretion of oxidized DNA/RNA bases with the hemin diet, revealing that rats were undergoing an oxidative genotoxic process (Fig. 4C), related to the observed 8-OHdG increase in the colon of hemin-fed rats. Oxidative stress is known to induce base lesions and single-strand DNA breaks (Kryston *et al.* 2011). Taken together, those results could explain the co-initiating effect of the hemin diet observed in the present study, involving a heme-induced lipid peroxidation/oxidative stress process.

In the present study, the effect of the iron diets on inflammation parameters was diverse. For local colon parameters, a significant reduction of colon length with the hemin diet was observed at the end of the protocol but not just after the 2-week dietary period, indicating a possible inflammatory process. The reduction of colon length has been reported by many authors as an effect of DSS treatment provoking colon inflammation

Downloaded from Bioscientifica.com at 07/22/2025 01:00:31PM
via Open Access. This work is licensed under a Creative Commons
Attribution-NonCommercial-NoDerivatives 4.0 International License.
https://creativecommons.org/licenses/by-nc-nd/4.0/

(Ahn *et al.* 2020). On the other side, IL-1β protein was significantly decreased by this diet. *Cox2* expression, an inducible marker of inflammation, and microscopic injury score were non-statistically significantly increased by the hemin diet (Fig. 5B). Systemic parameters, namely plasmatic MPO, CRP and urinary 8-isoPGF$_{2\alpha}$ were also diversely altered, with an increase in MPO with both ferric citrate and hemin diets, but no effect for CRP, and an increase in 8-isoPGF$_{2\alpha}$ effect (Fig. 5A) with the hemin diet, but this biomarker is also known to be representative of endogenous lipid peroxidation/oxidative stress. Altogether, these results are in favor of an oxidative stress process leading to a mild inflammation that, in our opinion, would not be sufficient to explain the effects of the hemin diet on preneoplastic lesions. Seiwert *et al.* in their work reported above with hemin-fed mice, reported a marked inflammation associated with weight loss of the animals (Seiwert *et al.* 2021). In the present study, we observed no weight loss and only mild change in some of the inflammation markers at the end of the experimental diet period. Other authors (Ijssennagger *et al.* 2015) and our group in an earlier work (Pierre *et al.* 2003) reported a significant 10% weight loss in hemin-fed mice and rats, respectively, when compared to control animals. The fact that we did not observe such weight loss in the present study, could be explained by the special care we currently take in feeding the rats, especially the time of day they are fed and the diet preparation methods, as mentioned in the Methods section, or by the duration of the experimental diets (only 2 weeks in the present study). This could also explain the only modest inflammation we observed.

We analyzed fecal microbiota composition by 16S rRNA sequencing. The hemin diet provoked a deep modification of microbiota structure and composition (Fig. 6), as reported in our earlier work (Martin *et al.* 2019), with a decrease in α-diversity and a modification of β-diversity, and for composition a decrease in *Firmicutes* and an increase in *Bacteroidetes* and *Proteobacteria.* These alterations are very close to those observed by Seiwert *et al.* in hemin-fed mice (Seiwert *et al.* 2021). Such a dysbiosis was reported to be related to CRC development, with an increase in *E. coli* and in *Bacteroides* and a decrease in *Lactobacilli* and *Bifidobacterium* (Janney *et al.* 2020). This dysbiosis is no longer observed when the hemin diet is stopped, indicating that the microbiota is able to be resilient and that the effect on preneoplastic lesions is not due to chronic dysbiosis.

Our results show for the first time that iron is able to co-initiate CRC in rats, but only in its heminic form, as we observed an increase of both types of preneoplastic lesions only with the hemin diet. The processes that are specific for this heminic form of iron are massive luminal lipid peroxidation that is associated with an important oxidative colon RNA/DNA damage, cytotoxicity of fecal waters, cell proliferation in colon mucosa, a reduction of protective mucus and increased urinary excretion of oxidative stress and genotoxicity biomarkers, together with a gut dysbiosis. The ferric citrate diet induced moderate lipid peroxidation, which is balanced by the induction of antioxidant defenses, with no effect on preneoplastic lesions or gut microbiota.

In the future, those results will need to be consolidated by performing a CRC initiation experiment without AOM in male and female animals, and long enough to reach the tumor stage. In order to decipher the roles of lipid peroxidation and/or of gut dysbiosis, specific studies with the use of lipid peroxidation products such as HNE or the use of antioxidants in the diet and the approach of fecal microbiota transfer will sure be of interest.

Supplementary materials

This is linked to the online version of the paper at https://doi.org/10.1530/REM-25-0001.

Declaration of interest

FG and FP have some research projects that have been co-financed by the processed meat sector. The results presented here are not part of these co-financed projects.

Funding

This research was funded by ITMO Cancer (Plan cancer 2009–2013)/INCa/INSERM for financial support (academic funding). JK's PhD was financially supported by the INRAE Human Nutrition department and EIP (Ecole d'Ingénieurs de Purpan).

Author contribution statement

Conceptualization was done by FG with JK, VT and FP. Methodology and experimentation were performed by JK, PP, EF, EMP, NN, FBE, CM, IA, SC, MHM, CHT, SP, MC, LK, MA, MO and FG. Formal analysis was conducted by JK, PP, SC, SP, MC, MA, MO and FG. Writing of the original draft was carried out by FG, JK, PP and MO. Writing review and editing were performed by VT, FP, PP, MO and FG. All authors read and approved the final manuscript.

Data availability

The raw data set (16S rRNA sequences) described in this project has been deposited in the MG-RAST database under accession code mgp101012 (reviewer access token: https://www.mg-rast.org/mgmain.html?mgpage=token&token=63dJTN7ZQ7jU4rwr7fdFRad6cGq8R2ayg6MNQHrUmWlOnfdbiO). Further information and requests for resources and reagents will be fulfilled by the corresponding author, FG.

Acknowledgments

We are grateful to the Get-PlaGe platform team (Toulouse, France) for 16S rDNA libraries and sequencing, the Genotoul bioinformatics platform Toulouse Midi-Pyrénées and Sigenae group for providing help and storage resources, thanks to Galaxy instance http://sigenae-workbench.toulouse.inra.fr. The authors would like to thank the MetaboHUB French National Infrastructure (MetaboHUB- ANR-11-INBS-0010, 2011) for the LC-MS/MS analyses.

Downloaded from Bioscientifica.com at 07/22/2025 01:00:31PM
via Open Access. This work is licensed under a Creative Commons
Attribution-NonCommercial-NoDerivatives 4.0 International License.
https://creativecommons.org/licenses/by-nc-nd/4.0/

References

Ahn S-I, Cho S & Choi N-J 2020 Effect of dietary probiotics on colon length in an inflammatory bowel disease–induced murine model: a meta-analysis. *J Dairy Sci* **103** 1807–1819. (https://doi.org/10.3168/jds.2019-17356)

Audebert M, Dolo L, Perdu E, *et al.* 2011 Use of the γH2AX assay for assessing the genotoxicity of bisphenol A and bisphenol F in human cell lines. *Arch Toxicol* **85** 1463–1473. (https://doi.org/10.1007/s00204-011-0721-2)

Bastide NM, Chenni F, Audebert M, *et al.* 2015 A central role for heme iron in colon carcinogenesis associated with red meat intake. *Cancer Res* **75** 870–879. (https://doi.org/10.1158/0008-5472.CAN-14-2554)

Bastide N, Morois S, Cadeau C, *et al.* 2016 Heme iron intake, dietary antioxidant capacity, and risk of colorectal adenomas in a large cohort study of French women. *Cancer Epidemiol Biomarkers Prev* **25** 640–647. (https://doi.org/10.1158/1055-9965.EPI-15-0724)

Bird RP 1987 Observation and quantification of aberrant crypts in the murine colon treated with a colon carcinogen: preliminary findings. *Cancer Lett* **37** 147–151. (https://doi.org/10.1016/0304-3835(87)90157-1)

Bouvard V, Loomis D, Guyton KZ, *et al.* 2015 Carcinogenicity of consumption of red and processed meat. *Lancet Oncol* **16** 1599–1600. (https://doi.org/10.1016/S1470-2045(15)00444-1)

Bray F, Ferlay J, Soerjomataram I, *et al.* 2018 Global cancer statistics 2018: GLOBOCAN estimates of incidence and mortality worldwide for 36 cancers in 185 countries. *CA Cancer J Clin* **68** 394–424. (https://doi.org/10.3322/caac.21492)

Cabelof DC, Raffoul JJ, Yanamadala S, *et al.* 2002 Induction of DNA polymerase beta-dependent base excision repair in response to oxidative stress in vivo. *Carcinogenesis* **23** 1419–1425. (https://doi.org/10.1093/carcin/23.9.1419)

Caderni G, Femia AP, Giannini A, *et al.* 2003 Identification of mucin-depleted foci in the unsectioned colon of azoxymethane-treated rats: correlation with carcinogenesis. *Cancer Res* **63** 2388–2392.

Chevolleau S, Noguer-Meireles M-H, Jouanin I, *et al.* 2018 Development and validation of an ultra high performance liquid chromatography-electrospray tandem mass spectrometry method using selective derivatisation, for the quantification of two reactive aldehydes produced by lipid peroxidation, HNE (4-hydroxy-2(E)-nonenal) and HHE (4-hydroxy-2(E)-hexenal) in faecal water. *J Chromatogr B Analyt Technol Biomed Life Sci* **1083** 171–179. (https://doi.org/10.1016/j.jchromb.2018.03.002)

Clapper ML, Chang W-CL & Cooper HS 2020 Dysplastic aberrant crypt foci: biomarkers of early colorectal neoplasia and response to preventive intervention. *Cancer Prev Res* **13** 229–240. (https://doi.org/10.1158/1940-6207.CAPR-19-0316)

Clinton SK, Giovannucci EL & Hursting SD 2020 The World Cancer Research Fund/American Institute for Cancer Research Third Expert Report on Diet, Nutrition, Physical Activity, and Cancer: Impact and Future Directions. *J Nutr* **150** 663–671. (https://doi.org/10.1093/jn/nxz268)

Constante M, Fragoso G, Calvé A, *et al.* 2017 Dietary heme induces gut dysbiosis, aggravates colitis, and potentiates the development of adenomas in mice. *Front Microbiol* **8** 1809. (https://doi.org/10.3389/fmicb.2017.01809)

Corpet DE & Taché S 2002 Most effective colon cancer chemopreventive agents in rats: a systematic review of aberrant crypt foci and tumor data, ranked by potency. *Nutr Cancer* **43** 1–21. (https://doi.org/10.1207/S15327914NC431_1)

Csala M, Kardon T, Legeza B, *et al.* 2015 On the role of 4-hydroxynonenal in health and disease. *Biochim Biophys Acta* **1852** 826–838. (https://doi.org/10.1016/j.bbadis.2015.01.015)

Cui C, Takamatsu R, Doguchi H, *et al.* 2012 Pre-neoplastic lesion, mucin-depleted foci, reveals de novo high-grade dysplasia in rat colon carcinogenesis. *Oncol Rep* **27** 1365–1370. (https://doi.org/10.3892/or.2012.1657)

Dang H, Harryvan TJ & Hawinkels LJAC 2021 Fibroblast subsets in intestinal homeostasis, carcinogenesis, tumor progression, and metastasis. *Cancers* **13** 183. (https://doi.org/10.3390/cancers13020183)

de Vogel J, van-Eck WB, Sesink ALA, *et al.* 2008 Dietary heme injures surface epithelium resulting in hyperproliferation, inhibition of apoptosis and crypt hyperplasia in rat colon. *Carcinogenesis* **29** 398–403. (https://doi.org/10.1093/carcin/bgm278)

Dick RA, Kwak MK, Sutter TR, *et al.* 2001 Antioxidative function and substrate specificity of NAD(P)H- dependent alkenal/one oxidoreductase. *J Biol Chem* **276** 40803–40810. (https://doi.org/10.1074/jbc.M105487200)

Dupuy J, Cogo E, Fouché E, *et al.* 2024 Epithelial-mesenchymal interaction protects normal colonocytes from 4-HNE-induced phenotypic transformation. *PLoS One* **19** e0302932. (https://doi.org/10.1371/journal.pone.0302932)

Eckl PM 2003 Genotoxicity of HNE. *Mol Aspects Med* **24** 161–165. (https://doi.org/10.1016/s0098-2997(03)00010-4)

Eckl PM & Bresgen N 2017 Genotoxicity of lipid oxidation compounds. *Free Radical Biol Med* **111** 244–252. (https://doi.org/10.1016/j.freeradbiomed.2017.02.002)

Eckl PM, Ortner A & Esterbauer H 1993 Genotoxic properties of 4-hydroxyalkenals and analogous aldehydes. *Mutat Res* **290** 183–192. (https://doi.org/10.1016/0027-5107(93)90158-c)

Escudié F, Auer L, Bernard M, *et al.* 2017 FROGS: find, rapidly, OTUs with galaxy solution. *Bioinformatics* **34** 1287–1294. (https://doi.org/10.1093/bioinformatics/btx791)

Femia AP, Dolara P & Caderni G 2004 Mucin-depleted foci (MDF) in the colon of rats treated with azoxymethane (AOM) are useful biomarkers for colon carcinogenesis. *Carcinogenesis* **25** 277–281. (https://doi.org/10.1093/carcin/bgh005)

Femia AP, Bendinelli B, Giannini A, *et al.* 2005 Mucin-depleted foci have β-catenin gene mutations, altered expression of its protein, and are dose- and time-dependent in the colon of 1,2-dimethylhydrazine-treated rats. *Int J Cancer* **116** 9–15. (https://doi.org/10.1002/ijc.20981)

Femia AP, Dolara P, Giannini A, *et al.* 2007 Frequent mutation of Apc gene in rat colon tumors and mucin-depleted foci, preneoplastic lesions in experimental colon carcinogenesis. *Cancer Res* **67** 445–449. (https://doi.org/10.1158/0008-5472.CAN-06-3861)

Femia AP, Giannini A, Fazi M, *et al.* 2008 Identification of mucin depleted foci in the human colon. *Cancer Prev Res* **1** 562–567. (https://doi.org/10.1158/1940-6207.CAPR-08-0125)

Forest V, Clement M, Pierre F, *et al.* 2003 Butyrate restores motile function and actin cytoskeletal network integrity in apc mutated mouse colon epithelial cells. *Nutr Cancer* **45** 84–92. (https://doi.org/10.1207/S15327914NC4501_10)

Guan L, Wen T, Zhang Y, *et al.* 2009 Induction of heme oxygenase-1 with hemin attenuates hippocampal injury in rats after acute carbon monoxide poisoning. *Toxicology* **262** 146–152. (https://doi.org/10.1016/j.tox.2009.06.001)

Guéraud F 2017 4-Hydroxynonenal metabolites and adducts in pre-carcinogenic conditions and cancer. *Free Radical Biol Med* **111** 196–208. (https://doi.org/10.1016/j.freeradbiomed.2016.12.025)

Guéraud F, Peiro G, Bernard H, *et al.* 2006 Enzyme immunoassay for a urinary metabolite of 4-hydroxynonenal as a marker of lipid peroxidation.

Downloaded from Bioscientifica.com at 07/22/2025 01:00:31PM
via Open Access. This work is licensed under a Creative Commons
Attribution-NonCommercial-NoDerivatives 4.0 International License.
https://creativecommons.org/licenses/by-nc-nd/4.0/

Free Radic Biol Med **40** 54–62.
(https://doi.org/10.1016/j.freeradbiomed.2005.08.011)

Guéraud F, Atalay M, Bresgen N, *et al.* 2010 Chemistry and biochemistry of lipid peroxidation products. *Free Radic Res* **44** 1098–1124.
(https://doi.org/10.3109/10715762.2010.498477)

Guéraud F, Taché S, Steghens J-P, *et al.* 2015 Dietary polyunsaturated fatty acids and heme iron induce oxidative stress biomarkers and a cancer promoting environment in the colon of rats. *Free Radic Biol Med* **83** 192–200.
(https://doi.org/10.1016/j.freeradbiomed.2015.02.023)

IARC Working Group on the Evaluation of Carcinogenic Risk to Humans 2018 Red meat and processed meat. In *IARC Monographs on the Evaluation of Carcinogenic Risks to Humans*. Lyon, FR: International Agency for Research on Cancer.

Ijssennagger N, Rijnierse A, de Wit N, *et al.* 2012 Dietary haem stimulates epithelial cell turnover by downregulating feedback inhibitors of proliferation in murine colon. *Gut* **61** 1041–1049.
(https://doi.org/10.1136/gutjnl-2011-300239)

Ijssennagger N, Belzer C, Hooiveld GJ, *et al.* 2015 Gut microbiota facilitates dietary heme-induced epithelial hyperproliferation by opening the mucus barrier in colon. *Proc Natl Acad Sci U S A* **112** 10038–10043.
(https://doi.org/10.1073/pnas.1507645112)

Janney A, Powrie F & Mann EH 2020 Host–microbiota maladaptation in colorectal cancer. *Nature* **585** 509–517.
(https://doi.org/10.1038/s41586-020-2729-3)

Jawhara M, Sørensen SB, Heitmann BL, *et al.* 2020 The relation between red meat and whole-grain intake and the colonic mucosal barrier: a cross-sectional study. *Nutrients* **12** 1765.
(https://doi.org/10.3390/nu12061765)

Jayakumar S, Pal D & Sandur SK 2015 Nrf2 facilitates repair of radiation induced DNA damage through homologous recombination repair pathway in a ROS independent manner in cancer cells. *Mutat Res* **779** 33–45.
(https://doi.org/10.1016/j.mrfmmm.2015.06.007)

Kim DJ, Kang JS, Ahn B, *et al.* 2001 Chemopreventive effect of 2-(allylthio) pyrazine (2-AP) on rat colon carcinogenesis induced by azoxymethane (AOM). *Cancer Lett* **166** 125–133.
(https://doi.org/10.1016/S0304-3835(01)00408-6)

Kryston TB, Georgiev AB, Pissis P, *et al.* 2011 Role of oxidative stress and DNA damage in human carcinogenesis. *Mutat Res* **711** 193–201.
(https://doi.org/10.1016/j.mrfmmm.2010.12.016)

Lance P & Hamilton SR 2008 Sporadic aberrant crypt foci are not a surrogate endpoint for colorectal adenoma prevention. *Cancer Prev Res* **1** 4–8. (https://doi.org/10.1158/1940-6207.CAPR-08-0043)

Lê Cao K-A, Costello M-E, Lakis VA, *et al.* 2016 MixMC: a multivariate statistical framework to gain insight into microbial communities. *PLoS One* **11** e0160169. (https://doi.org/10.1371/journal.pone.0160169)

Lee J, Yesilkanal AE, Wynne JP, *et al.* 2019 Effective breast cancer combination therapy targeting BACH1 and mitochondrial metabolism. *Nature* **568** 254–258. (https://doi.org/10.1038/s41586-019-1005-x)

Li L, Lu M, Peng Y, *et al.* 2023 Oxidatively stressed extracellular microenvironment drives fibroblast activation and kidney fibrosis. *Redox Biol* **67** 102868. (https://doi.org/10.1016/j.redox.2023.102868)

Liu R & Xu G 2008 Effects of resistant starch on colonic preneoplastic aberrant crypt foci in rats. *Food Chem Toxicol* **46** 2672–2679.
(https://doi.org/10.1016/j.fct.2008.04.038)

Lombardi-Boccia G, Martinez-Dominguez B & Aguzzi A 2002 Total heme and non-heme iron in raw and cooked meats. *J Food Sci* **67** 1738–1741.
(https://doi.org/10.1111/j.1365-2621.2002.tb08715.x)

Martin OCB, Naud N, Taché S, *et al.* 2018 Targeting colon luminal lipid peroxidation limits colon carcinogenesis associated with red meat consumption. *Cancer Prev Res* **11** 569–580.
(https://doi.org/10.1158/1940-6207.CAPR-17-0361)

Martin OCB, Olier M, Ellero-Simatos S, *et al.* 2019 Haem iron reshapes colonic luminal environment: impact on mucosal homeostasis and microbiome through aldehyde formation. *Microbiome* **7** 72.
(https://doi.org/10.1186/s40168-019-0685-7)

McMurdie PJ & Holmes S 2012 Phyloseq: a bioconductor package for handling an analysis of high-throughput phylogenetic sequence data. *Pac Symp Biocomput* 235–246.

McMurdie PJ & Holmes S 2013 Phyloseq: an R package for reproducible interactive analysis and graphics of microbiome census data. *PLoS One* **8** e61217. (https://doi.org/10.1371/journal.pone.0061217)

Menegon S, Columbano A & Giordano S 2016 The dual roles of NRF2 in cancer. *Trends Mol Med* **22** 578–593.
(https://doi.org/10.1016/j.molmed.2016.05.002)

Nishizawa H, Yamanaka M & Igarashi K 2023 Ferroptosis: regulation by competition between NRF2 and BACH1 and propagation of the death signal. *FEBS J* **290** 1688–1704.
(https://doi.org/10.1111/febs.16382)

Ohkawa H, Ohishi N & Yagi K 1979 Assay for lipid peroxides in animal tissues by thiobarbituric acid reaction. *Anal Biochem* **95** 351–358.
(https://doi.org/10.1016/0003-2697(79)90738-3)

Peiro G, Alary J, Cravedi J-P, *et al.* 2005 Dihydroxynonene mercapturic acid, a urinary metabolite of 4-hydroxynonenal, as a biomarker of lipid peroxidation. *Biofactors* **24** 89–96.
(https://doi.org/10.1002/biof.5520240110)

Pierre F, Taché S, Petit CR, *et al.* 2003 Meat and cancer: haemoglobin and haemin in a low-calcium diet promote colorectal carcinogenesis at the aberrant crypt stage in rats. *Carcinogenesis* **24** 1683–1690.
(https://doi.org/10.1093/carcin/bgg130)

Pierre F, Taché S, Corpet DE, *et al.* 2004 Beef meat and blood sausage promote the formation of azoxymethane-induced mucin-depleted foci and aberrant crypt foci in rat colons. *J Nutr* **134** 2711–2716.
(https://doi.org/10.1093/jn/134.10.2711)

Pierre F, Tache S, Gueraud F, *et al.* 2007 Apc mutation induces resistance of colonic cells to lipoperoxide-triggered apoptosis induced by faecal water from haem-fed rats. *Carcinogenesis* **28** 321–327.
(https://doi.org/10.1093/carcin/bgl127)

Pierre F, Santarelli R, Taché S, *et al.* 2008 Beef meat promotion of dimethylhydrazine-induced colorectal carcinogenesis biomarkers is suppressed by dietary calcium. *Br J Nutr* **99** 1000–1006.
(https://doi.org/10.1017/S0007114507843558)

Plaisancié P, Buisson C, Fouché E, *et al.* 2022 Study of the colonic epithelial-mesenchymal dialogue through establishment of two activated or not mesenchymal cell lines: activated and resting ones differentially modulate colonocytes in co-culture. *PLoS One* **17** e0273858.
(https://doi.org/10.1371/journal.pone.0273858)

Poulsen M, Mølck A-M, Thorup I, *et al.* 2001 The influence of simple sugars and starch given during pre- or post-initiation on aberrant crypt foci in rat colon. *Cancer Lett* **167** 135–143.
(https://doi.org/10.1016/S0304-3835(01)00487-6)

R Development Core Team 2011 *R: A language and environment for statistical computing*. R Foundation for Statistical Computing, Vienna, Austria.
(https://www.r-project.org/)

Sánchez-Rodríguez R, Torres-Mena JE, Quintanar-Jurado V, *et al.* 2017 Ptgr1 expression is regulated by NRF2 in rat hepatocarcinogenesis and promotes

Downloaded from Bioscientifica.com at 07/22/2025 01:00:31PM
via Open Access. This work is licensed under a Creative Commons
Attribution-NonCommercial-NoDerivatives 4.0 International License.
https://creativecommons.org/licenses/by-nc-nd/4.0/

cell proliferation and resistance to oxidative stress. *Free Radical Biol Med* **102** 87–99. (https://doi.org/10.1016/j.freeradbiomed.2016.11.027)

Segata N, Izard J, Waldron L, *et al.* 2011 Metagenomic biomarker discovery and explanation. *Genome Biol* **12** R60. (https://doi.org/10.1186/gb-2011-12-6-r60)

Seiwert N, Adam J, Steinberg P, *et al.* 2021 Chronic intestinal inflammation drives colorectal tumor formation triggered by dietary heme iron in vivo. *Arch Toxicol* **95** 2507–2522. (https://doi.org/10.1007/s00204-021-03064-6)

Sesink AL, Termont DS, Kleibeuker JH, *et al.* 1999 Red meat and colon cancer: the cytotoxic and hyperproliferative effects of dietary heme. *Cancer Res* **59** 5704–5709.

Sesink ALA, Termont DSML, Kleibeuker JH, *et al.* 2000 Red meat and colon cancer: dietary haem, but not fat, has cytotoxic and hyperproliferative effects on rat colonic epithelium. *Carcinogenesis* **21** 1909–1915. (https://doi.org/10.1093/carcin/21.10.1909)

Sesink AL, Termont DS, Kleibeuker JH, *et al.* 2001 Red meat and colon cancer: dietary haem-induced colonic cytotoxicity and epithelial hyperproliferation are inhibited by calcium. *Carcinogenesis* **22** 1653–1659. (https://doi.org/10.1093/carcin/22.10.1653)

Stevens RG, Pretlow TP, Hurlstone DP, *et al.* 2008 Comment re: "Sporadic aberrant crypt foci are not a surrogate endpoint for colorectal adenoma prevention" and "Aberrant crypt foci in the adenoma prevention with celecoxib trial". *Cancer Prev Res* **1** 215–216. (https://doi.org/10.1158/1940-6207.CAPR-08-0094)

Stocker P, Cassien M, Vidal N, *et al.* 2017 A fluorescent homogeneous assay for myeloperoxidase measurement in biological samples. A positive correlation between myeloperoxidase-generated HOCl level and oxidative status in STZ-diabetic rats. *Talanta* **170** 119–127. (https://doi.org/10.1016/j.talanta.2017.03.102)

Takayama T, Katsuki S, Takahashi Y, *et al.* 1998 Aberrant crypt foci of the colon as precursors of adenoma and cancer. *N Engl J Med* **339** 1277–1284. (https://doi.org/10.1056/NEJM199810293391803)

Tudek B, Bird RP & Bruce WR 1989 Foci of aberrant crypts in the colons of mice and rats exposed to carcinogens associated with foods. *Cancer Res* **49** 1236–1240.

Van der Sluis M, De Koning BAE, De Bruijn ACJM, *et al.* 2006 Muc2-deficient mice spontaneously develop colitis, indicating that MUC2 is critical for colonic protection. *Gastroenterology* **131** 117–129. (https://doi.org/10.1053/j.gastro.2006.04.020)

Vieira AR, Abar L, Chan DSM, *et al.* 2017 Foods and beverages and colorectal cancer risk: a systematic review and meta-analysis of cohort studies, an update of the evidence of the WCRF-AICR Continuous Update Project. *Ann Oncol* **28** 1788–1802. (https://doi.org/10.1093/annonc/mdx171)

Wiel C, Le Gal K, Ibrahim MX, *et al.* 2019 BACH1 stabilization by antioxidants stimulates lung cancer metastasis. *Cell* **178** 330–345.e22. (https://doi.org/10.1016/j.cell.2019.06.005)

Worou M-E, Belmokhtar K, Bonnet P, *et al.* 2011 Hemin decreases cardiac oxidative stress and fibrosis in a rat model of systemic hypertension via PI3K/Akt signalling. *Cardiovasc Res* **91** 320–329. (https://doi.org/10.1093/cvr/cvr072)

Downloaded from Bioscientifica.com at 07/22/2025 01:00:31PM
via Open Access. This work is licensed under a Creative Commons
Attribution-NonCommercial-NoDerivatives 4.0 International License.
https://creativecommons.org/licenses/by-nc-nd/4.0/